PARTICULATE INGRESSION PAST ELASTOMERIC

VISCOELASTIC LINEAR MOTION SEALS

By

DEAN HAROLD AHLBERG

Bachelor of Mechanical Engineering

University of Minnesota
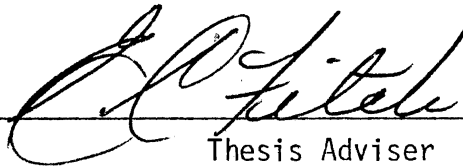
Minneapolis, Minnesota

1978

Submitted to the Faculty of the Graduate College
of the Oklahoma State University
in partial fulfillment of the requirements
for the Degree of
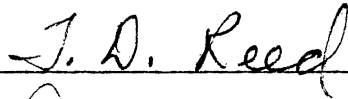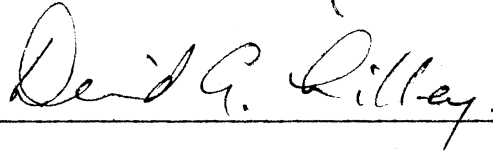MASTER OF SCIENCE
December, 1980

PARTICULATE INGRESSION PAST ELASTOMERIC

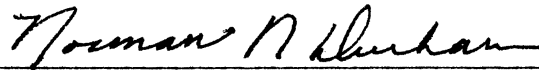VISCOELASTIC LINEAR MOTION SEALS

Thesis Approved:

E. C. Fitch
Thesis Adviser

J. D. Reed

David G. Lilley.

Norman N. Durham
Dean of Graduate College

PREFACE

This study is concerned with the problem of particulate ingression past linear elastomeric seals of the type used in hydraulic linear actuators. The primary objective of this study was to identify and explain the mechanism whereby particulates are able to be carried past the interface of an elastomeric seal and its metal mating surface. The main parameters determining this particulate transport past the elastomer-mating-surface interface are identified and the mechanism of these parameters on particulate transport are explained. A theory of particulate transport past elastomeric linear seals has been developed and experimental evidence is offered of its correctness.

The author wishes to thank his major adviser, Dr. E. C. Fitch, for his help and interest throughout the course of this study. The author's association with Dr. Fitch as both adviser and employer has been both pleasant and rewarding.

The author also wishes to thank other members of his committee, Dr. David Lilley and Dr. Troy Reed, for their willingness in offering their valuable criticism of this study. The author has had the privilege of taking course work under both of these fine professors. The author is especially indebted to Dr. Reed for his persistance in convincing his students never to accept any

TABLE OF CONTENTS

LIST OF TABLES

LIST OF FIGURES

NOMENCLATURE

a_1, a_2 radii of curvature of the meniscus

a_0 semi-length of particulate-elastomer contact

C   circumference of the mating surface

d   perpendicular distance from particulate center line to point of initial elastomer-particulate contact

d_s/d_{ACFTD} ratio of spherical to ACFTD particulates

d   particle diameter

D, d_r diameter of the mating surface

d_s seal cross-sectional diameter

d_b bore diameter

E'   dynamic Young's modulus

E_1, E_2 elastomer moduli

F_A normal force of elastomer on a particulate

F_T transmitted particulate force due to capillarity

F_H tangential force of mating-surface on particulate

F_N normal force of mating-surface on particulate

F(t)   normal force on particulate by the elastomer

F_C adhesion force due to capillarity

$F_{C,1}$ surface tension meniscus portion of the capillarity force

$F_{C,2}$ pressure deficit portion of the capillarity force

f_{rr} coefficient of rolling resistance

$F_{N,C}$ normal force on particulate due to capillarity

F   addition force on lead particulate

t	time
T	time for a particulate to move a distance equal to its semi-length of contact
T	time between the first and second appearance of a particle
$U[t - \sigma]$	Heaviside function
V_B	velocity of point B
V_A	velocity of point A
V	particulate velocity
W	normal load by elastomer on particulate
x	location of points of particulate-elastomer contact
x_0	point where the elastomer relinquishes contact with the particulate
y_0	a length along an infinitely long cylindrical particulate
z_0	maximum depth of particulate indentation
z	depth of particulate identation
μ	the coefficient between particulate and mating-surface coefficient of rolling friction
μ_{min}	minimum necessary particulate-mating-surface coefficient of friction to initiate particulate movement
μ_{max}	maximum necessary particulate-mating-surface coefficient of friction to initiate particulate movement
μ_c	minimum necessary friction coefficient between particulate and mating surface when capillarity is present
μ_p	particulate-particulate coefficient of friction
θ	the angle at which the elastomer meets the particle
σ	surface tension
σ	elastomer stress

F_{CP}	force between particulates due to capillarity
F	rolling resistance
h	verticle distance normal to the mating surface to the point of initial elastomer-particle contact
G	spring constant
k	relaxation time divided by the time taken for a particulate to move a distance equal to its semi-length of contact
k_c	π-term
ℓ	distance from the instant center of particulate rotating to mating surface
ℓ	elastomer thickness
ℓ	length of elastomer contact with the mating surface
ℓ_s	stroke length minus an error term
L	stroke length
M	moment on a particulate
N	number of particulates in a particulate sheet
n	particulate location from the end particulate
P_c	pressure deficit
P_c	contact pressure
R	number of particles 10 micrometers or larger passing the elastomer mating surface interface per foot of cycling distance
r	particulate radius
s	area of contact
S	percent squeeze on the elastomer
$\tan \delta$	loss tangent

α	angle of meniscus action
α	hysteresis loss factor
π	non-dimensional grouping
ω	angular velocity of a particulate
ω	circular frequency
ε	energy loss per cycle
$\phi(t - \sigma)$	relaxation function
ϕ	elastic energy input
τ	relaxation time
η	viscosity

CHAPTER I

INTRODUCTION

The use of hydraulics in modern life is astounding. Almost any machine, the size of a garden tractor or larger, incorporates several hydraulic systems. Most hyraulic systems contain at least one linear actuator. Every linear actuator depends on linear elastomeric seals to keep fluid in and particulate contamination out. The ingression of particulates past the seals of linear actuators has long been known to be the main source of contaminant ingression in a hydraulic system. The harm of particulate contaminants to hydraulic system life and oper-- ation has focused the interests of all who work with such systems on the problem of excluding particulate ingression past linear elastomeric seals. It is the intent of this study to propose a theory which effec- tively explains the mechanism of particulate ingression past linear elastomeric seals.

An exhaustive review of the subject of particulate ingression past linear seals was conducted and with this as a basis, sound theory was developed which is supported by experiment. The major resistance to the transport of particulates past linear elastomeric seals is shown to be due to the entrance zone geometry of linear seals and to the visco- elastic properties of the elastomers.

CHAPTER II

TRANSPORT OF PARTICULATES PAST
ELASTOMERIC LINEAR SEALS

This chapter is a review of the previous work, done on the problem
of particulate migration past elastomeric seals. It serves as a basis
for this study, a jumping off point for further theoretical development
of important concepts and for experimental work as well as for exposing
areas of neglect in need of exploration.

The angle which the elastomer makes with its mating surface, called
a chamfer angle, is considered a critical design parameter [1]. Figure
1 shows this angle, which faces away from the side of the elastomer
facing particulates, and another angle, called a cutback angle, which is
not considered a critical paramter in designing a seal to resist par-
ticulate transport. Cutback angles do influence elastomer strength
and also result in a buildup of particulates in front of the elastomer.

The pressure due to elastic interference of the elastomer with its
mating surface is considered an important parameter in controlling
particulate transport [2]. This pressure is thought to determine
whether or not particulates will be able to wedge themselves between
the elastomer and its mating surface. The width of contact between
elastomer and mating surface is not considered a critical parameter.
It is said that this distance should be of a certain width to act as
a support for the leading edge so that it is not folded inward by
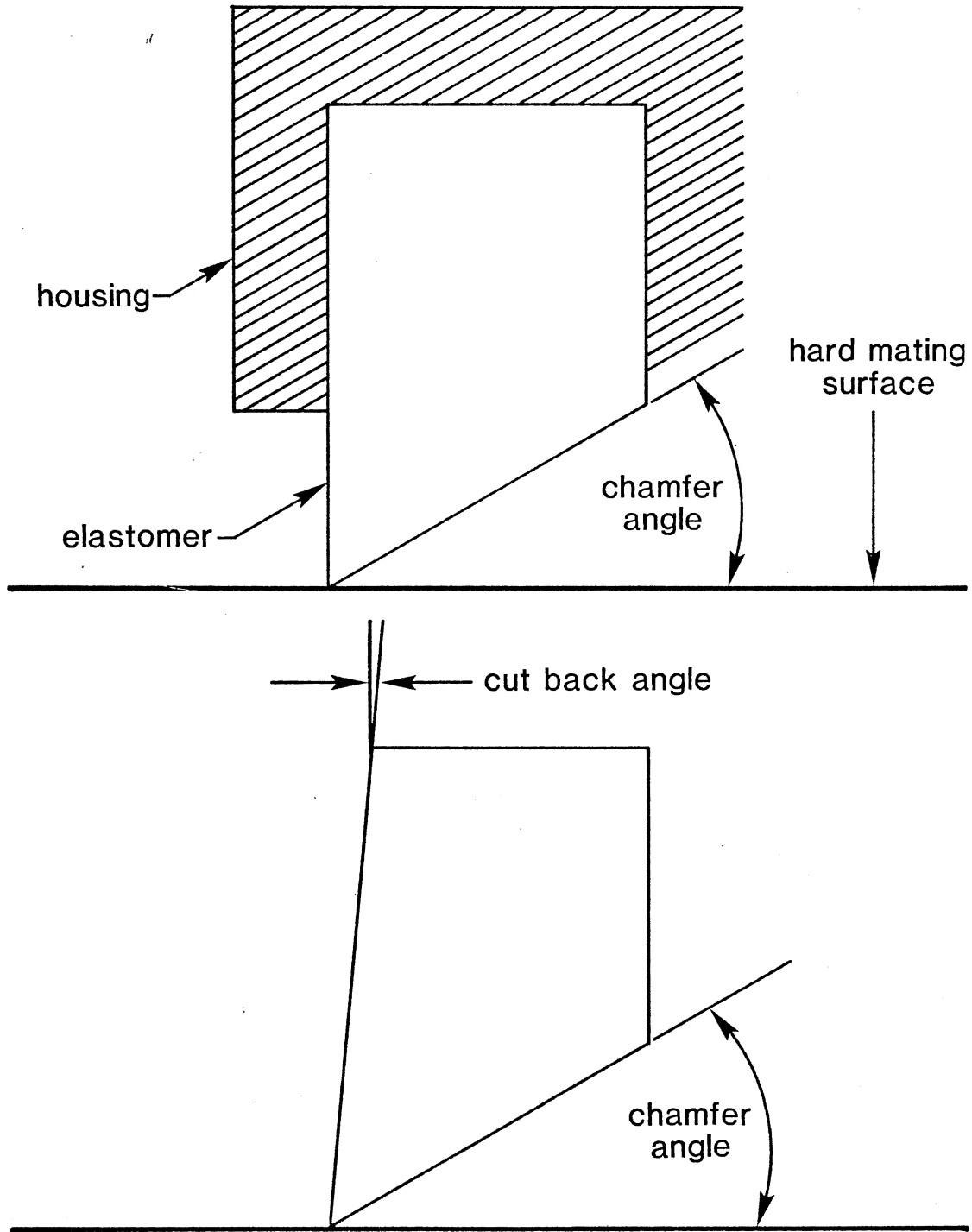
Figure 1. Angles Which Are Critical Design Parameters.

particulates. An elastomer-mating surface combination exposed to
particulate slurries is said to pass more particulates than when
exposed to any other form of particulate concentration.

The size of particulates is considered an important parameter
as to their ability to transit the elastomer-mating-surface inter-
face [3]. It is said that particulates 0.05 micrometre in size and
smaller pass easily beneath the elastomer with the thin film of fluid,
approximately 0.25 to 3.750 micrometers thick, present beneath the
mating surfaces and that particles of this size are not "felt". In-
creasing pressure between the interfaces is stated to be a way to reduce
the passage of particulates as well as using smoother surfaces. The
speed and direction of relative motion between the elastomer and its
mating surface is thought to be an important parameter influencing
particulate passage.

An experimental study was conducted showing the importance of
increasing the pressure between the mating surface due to elastic
compression of the elastomer [4]. The test placed a mud slurry on one
side of the elastomer. Its mating surface was then moved back and
forth for several hours, the mud passing from the slurry side of
the elastomer to the clean side. It was found that increasing the
elastic interference of the mating surfaces resulted in a decrease
in the rate at which mud passed through from one side to the other.
The material of the elastomer was found to be a variable in determining
the mud passage rate. Nitrile and polyurethane of equal Young's modulus
allowed mud to pass at different rates for the same amount of elastic
interference.

elastomer, per foot of cycled distance was found to be determined by an exponential expression of the form given by Eq. (2-1).

$$R = Ce^{ab} \tag{2-1}$$

where

R = the number of particles of size 19 micrometers of larger passing through the elastomer-mating-surface interface per foot of cycling distance;

C = constant which is experimentally determined;

a = constant which is experimentally determined;

b = the total distance of all the relative motion between the elastomer-mating-surface interface.

A typical equation for one of these seals is shown by Eq. (2-2).

$$R = 36e^{(2.4 \times 10^{-6}/foot)b} \tag{2-2}$$

In a further study with the same type of wiping seal, the amount of airborne contaminant was found to influence the number of particulates passing through the elastomer-mating-surface interface [7].

In a additional study, two differently designed wiping seals were tested under identical conditions with the only variable being the concentration of airborne particulates [8]. At one concentration level they passed similar quantities of particles larger than 10 micrometers in size. At different airborne particle concentration levels they passed very different quantities of particles larger than 10 micormeters in size.

The statement is made that elastomeric seals may trap particulates and that this phenomenon is dependent on the shape of the elastomers cross-section [9]. The pressure variations between the elastomer and its mating surface due to elastic interference is said

The film of fluid which forms beneath an elastomer and its mating surface during relative motion when a liquid is present has been measured for elastomeric seals of a square cross sectional shape [5]. The range was found to vary from between 0.05 micrometers to 4.0 micrometers in thickness. The thickness of the fluid film depends on fluid viscosity, speed of relative motion, elastomer geometry - especially the geometry in the region where fluid first enters between the elastomer and its mating surface - and the degree of elastic interference. Though thicker films are predicted for seals of different cross-section from that of square, none thicker have been measured. Thus particles larger than 4 micrometers in size are not likely to pass between the elastomer and its mating surface by being entrained in the thin fluid film. The statement is then made that particles normally of a size able to be sized and counted by automatic electronic particle counters will not very likely pass between the elastomer-mating-surface interface until the elastomer has degraded to the point where a film of fluid thick enough to entrain countable particles forms between it and its mating surface. These observations on particle passage are purely theoretical with no experimental evidence being presented.

A purely experimental study was performed in which an elastomeric seal of special shape designed to limit particulate transport (called a "wiper" in the hydraulics industry) was exposed, on one side, to airborne dust of known material, shape, and concentration while the other side was exposed to a film of oil carried by the rod as it moved through the seal [6]. The number of particles greater in size than 10 micrometers, passing from the air to the liquid side of the

to be related to the ability of the seal to push particles out of its way. It is also stated that the shape of the seal prior to the point where it contacts its mating surface and just behind this point of initial contact affects the ability of the seal to restrict the transport of particles between it and its mating surface. It was found by Bensch and Fitch [10] that hydraulic pressure seals which leak more, ingress fewer particulates than seals which leak less.

A delineated summary of this chapter is in order since the points brought out in this chapter will serve as the basis for further theoretical and experimental investigations:

1) Pressure variations between the elastomer and its mating surface due to elastic interference influences the transport of particulates between the interface.

2) The width of the elastomer-mating surface interface is not considered an important influence on particle transport.

3) Particulate slurries are said to be able to pass more particulates than other particle concentrations.

4) Particle size is deemed important to its ability to transit the interface.

5) The speed at which relative motion occurs between the elastomer and its mating surface is considered an important parameter influencing particle transport.

6) Elastomer material properties are shown to influence particulate transport.

7) The thickness of the film of oil between the elastomer and the mating surface is considered an important in-

fluence on particulate transport.

8) Particle transport through the elastomer-mating-surface interface is influenced by the level of airborne particulate concentration and the rate of such transport increased exponentially with the cycled distance of relative motion.

9) Elastomer geometry where contact between the elastomer and its mating surfaces begins is said to influence particulate transport.

10) Leaking seals allow less ingression of particulates than non-leaking seals.

CHAPTER III

SEAL EDGE GEOMETRY: THE ENTRANCE ZONE REGION

Of the ten items outlined in the last Chapter, which influence
the transport of particulates between the elastomer and its mating
surface, the geometry in the region where the seal initiates contact
with its mating surface was listed as number nine. This region of the
elastomer will be termed the "entrance zone". Its order in the listing
has no relation to the importance of its effect on the particulate
transport phenomenon. The entrance zone region of a seal must first
be crossed by any particle before it may enter that area between the
elastomer and its mating surface which is firmly pressed together
when no relative motion is taking place between them. This region
of intimate elastomer-mating-surface contact next to the entrance
zone will be termed the "interfacial zone".

The entrance zone acts on particulates in a very different manner
from that of the interfacial zone. In the interfacial zone, forces
act on the particle which are due to both displacement of the elastomer
by the particle and which are due to gross elastic interference
of the elastomer with its mating surface. This additional force
in the interfacial zone is a hydrostatic pressure force due to the
fact that the Poisson's ratio for a typical elastomer is approximately
0.50. The entrance zone also differs from the interfacial zone in
that it produces forces on particulates in a direction opposing their

9

motion toward the interfacial zone whether relative motion between the elastomer and its mating surface occurs or not. This is seen in Figure 2 where a cylinder of infinite length is assumed to model a particulate, a useful simplification to make understandable some important observations.

In Figure 2, a force balance on a free body of the model particulate is shown at the instant contact is made with the elastomer. The particle is assumed inertialess, which is a resonable assumption considering its small mass. The two points of contact are those of the elastomer - at the point where the force F_A acts on the particle - and the mating surface - at the point where the force F_N acts on the particle. The elastomer slope is always changing, growing smaller as the interfacial zone is approached. At the point of contact however, its variation over small distances, such as the diameter of particulates, may be considered negligible as the elastomer begins to drape over the particle.

As can be seen in Figure 2,

$$F_A \cos\theta = F_N \qquad (3\text{-}1)$$

$$F_A \sin\theta = F_H \qquad (3\text{-}2)$$

$$F_H \leq F_N \mu \qquad (3\text{-}3)$$

where μ is the coefficient of friction between the particulate-mating-surface interface.

Assuming the elastomer offers maximum resistance to the particulate,

$$F_A \sin\theta = F_A \cos\theta \mu \qquad (3\text{-}4)$$

$$\tan \theta = \mu \qquad (3\text{-}5)$$

Eq. (3-5) shows that if the coefficient of friction between the particu-

slope of elastomer at
point of initial contact

F_A

FREE BODY

d

θ

h

θ

F_H

F_N
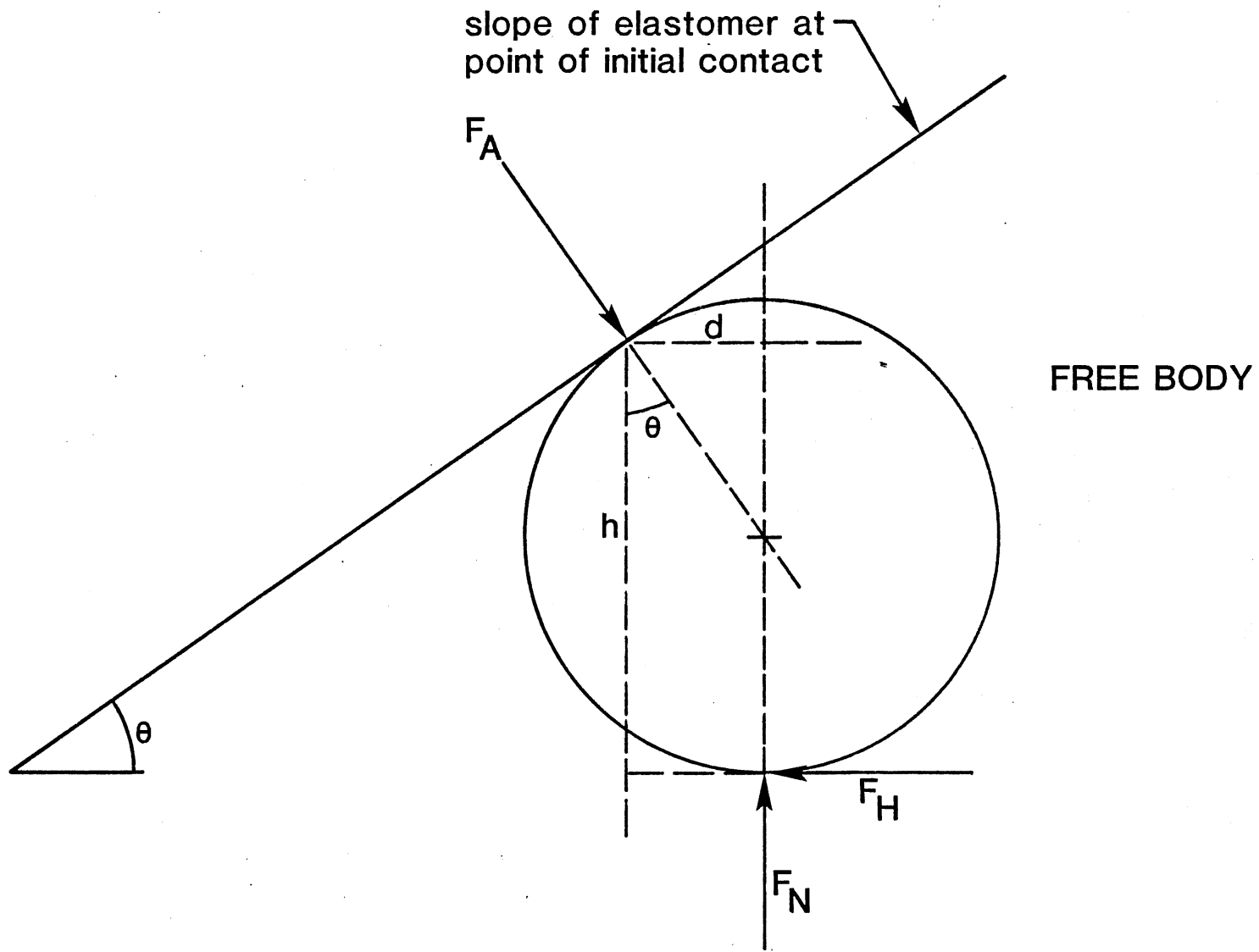
Figure 2. Initial Contact Between a Particulate and the Entrance Zone of a Seal.

late and the mating-surface exceeds the tangent of the slope of the elastomer at the point where it makes initial contact with the particulate, the particulate will be able to proceed toward the interfacial zone. Since the slope of the elastomer is always decreasing toward the interfacial zone, if the particulate is able to proceed after its initial contact with the elastomer, it will continue to proceed into the interfacial zone.

Actually, the coefficient of friction may be close to one-half the value found in Eq. (3-5) and still be sufficient to allow the particulate to move into the interfacial zone. If the moments on the particulate are summed about any point and set equal to zero, the horizontal force, F_H, just sufficient to cause the particulate to roll will be found. A point of interest about friction forces, such as F_H, is that such forces may vary from zero up to a maximum value. Thus, as shown by Eq. (3-3), F_H is at the most equal to $F_N\mu$. Since F_H need not equal $F_N\mu$, the coefficient of friction, μ, may be less than the value given by Eq. (3-5). Summing the moments:

$$F_N d - F_H h = 0 \tag{3-6}$$

where $d/h = F_H/F_N \leq \mu$

$$d/h = F_H/F_N \leq \mu \tag{3-7}$$

Since

$$h = r(1 + \cos\theta) \tag{3-8}$$

and

$$d = r\sin\theta \tag{3-9}$$

$$d/h = \sin\theta/(1 + \cos\theta) \leq \mu \tag{3-10}$$

and therefore the minimum μ is

$$\sin\theta/(1 + \cos\theta) = \mu_{min} < \mu_{max} = \tan\theta \qquad (3-11)$$

or

$$\tan\theta/(1 + \sec\theta) = \mu_{min} \qquad (3-12)$$

Thus the minimum coefficient of friction needed to intiate particulate movement in the entrance zone is $(1 + \sec\theta)^{-1}$ times as large as the slope of the elastomer at that point. Figure 3 is a graph of the minimum friction coefficient and $\tan\theta$ versus the angle of initial contact. It is seen that the minimum friction coefficient necessary for initiation of particulate transfer for the model particulate is approximately 1/2 $\tan\theta$. Also, Figure 3 shows that the minimum coefficient of friction never exceeds 1.
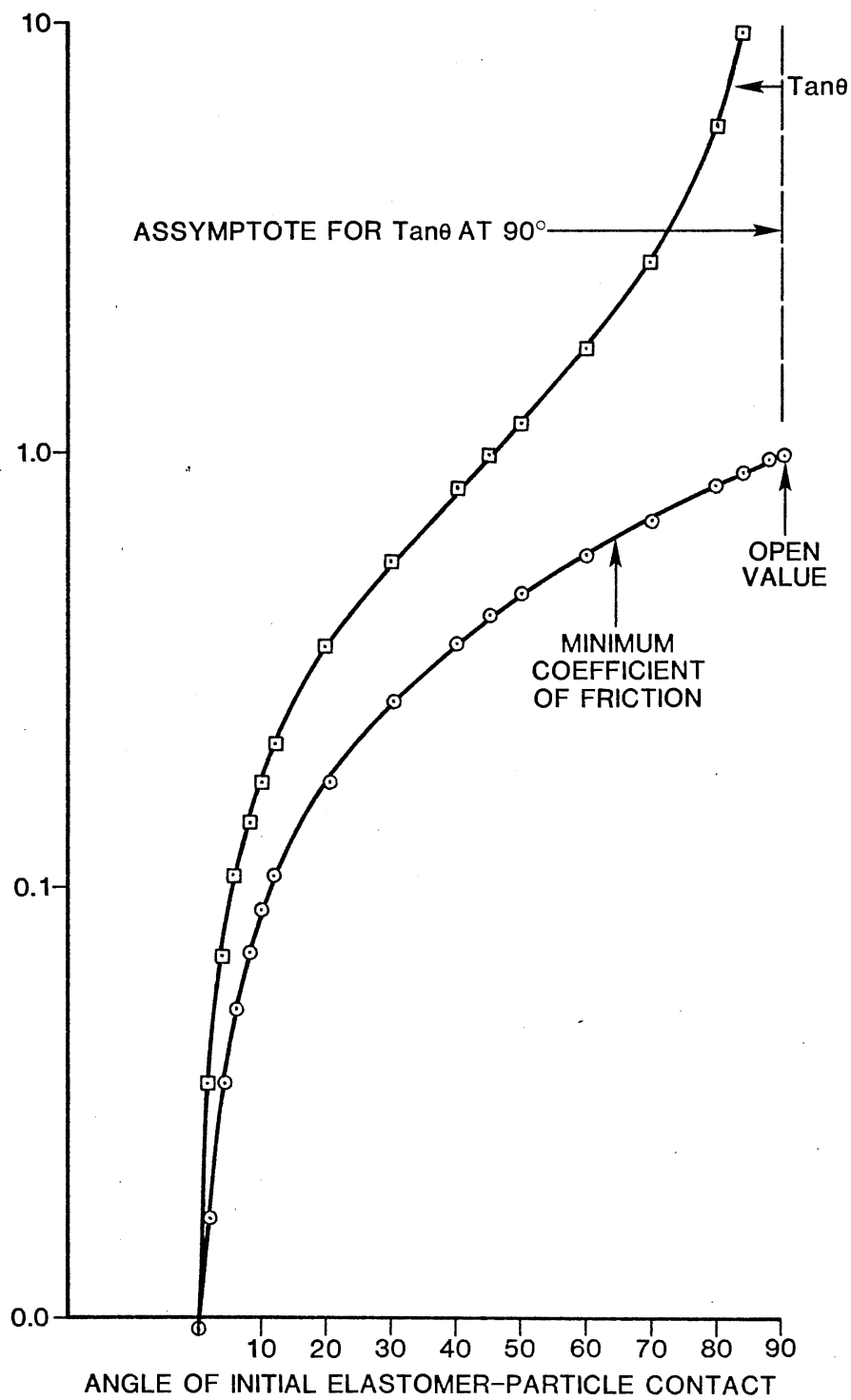
Figure 3. The Necessary Coefficient of Friction
Between Particulate and Mating Surface
to Initiate Movement.

CHAPTER IV

CAPILLARITY: ITS EFFECT ON SINGLE

PARTICULATES IN THE ENTRANCE ZONE

In Chapter III, the necessary coefficients of friction between
particulates and the mating surface for particulates of cylindrical or
spherical shape which allow them to proceed toward the interfacial
zone upon contact with the elastomer were calculated. The last
chapter dealt with single particles which were assumed to roll on
the elastomer surface upon coming into contact with it. If more than
one particulate at a time moves toward the entrance zone, the analysis
in the last chapter may not be sufficient to predict whether or not
particulates will move along the entrance zone. When particulates
form a sheet of closely contacting particles, the force picture is
altered on the particulates as they initiate contact with the elastomer.
The additional forces assisting particulate movement in the entrance
zone come from capillarity effects.

Figure 4 shows two spherical particles in close contact with
fluid deposited in and around their interface. [1] The meniscus pro-
duces an adhesion force on the particles due to surface tension and
the concavity of the liquid layer reduces its pressure below that
of the ambient surrounding air producing an additional adhesional

_____

[1]This analysis follows closely that of Zimon, Ref. [11].

15
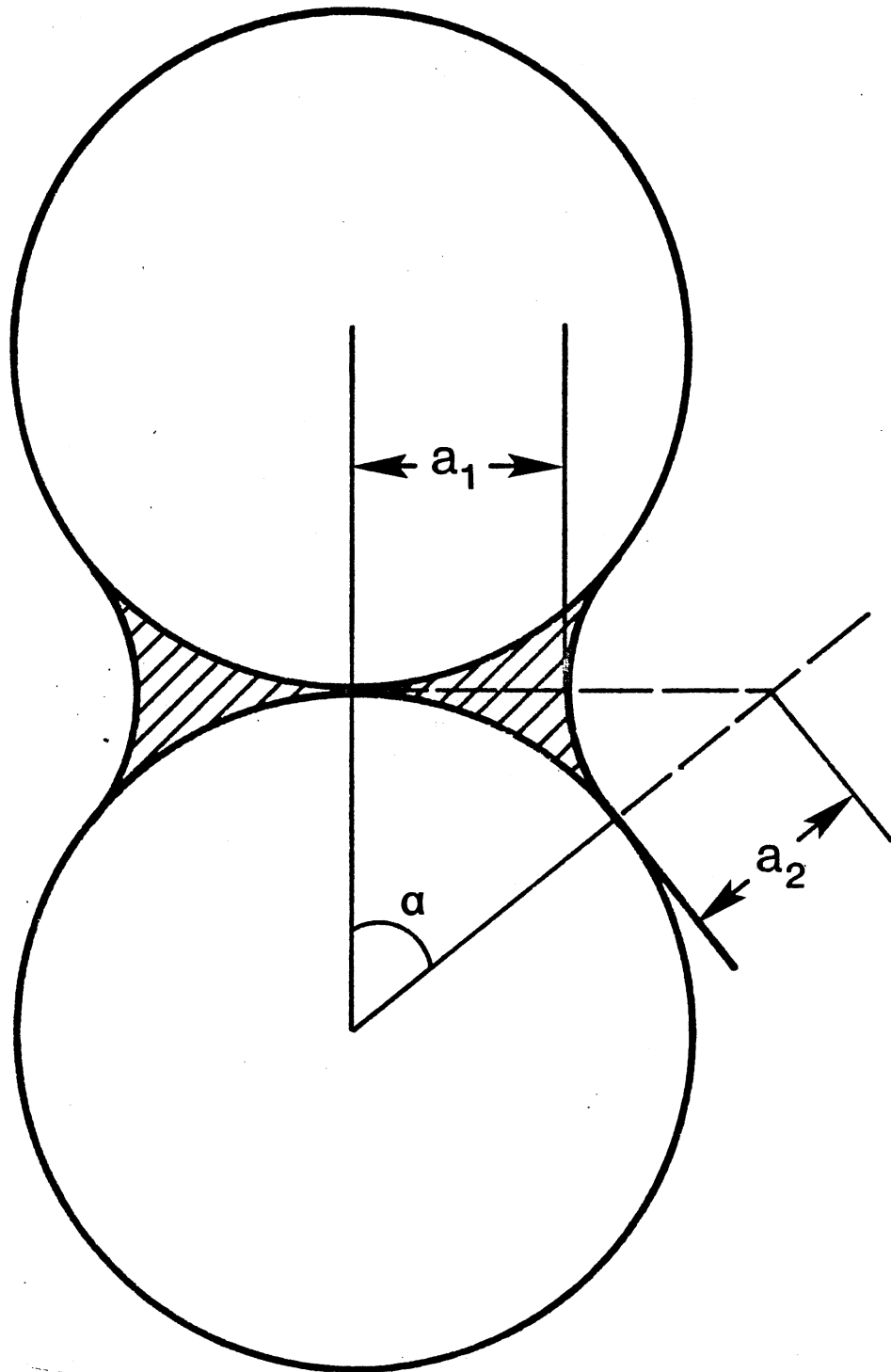
Figure 4. The Effect of Capillarity on Spherical
Particulates.

force. The forces on each particle are

$$F_c = F_{c,1} - F_{c,2} \tag{4-1}$$

where F_c = the adhesion force due to capillarity;

$F_{c,1}$ = the surface tension meniscus portion of the capillarity;

$F_{c,2}$ = the pressure deficit portion of the capillarity force.

$$F_{c,1} = 2\pi a_1 \sigma \tag{4-2}$$

where a_1 = a radii of curvature of the meniscus;

σ = surface tension of the fluid.

$$F_{c,2} = SPc \tag{4-3}$$

where S = area of contact;

P_c = pressure dificit which is a negative value.

$$s = \pi a_1^2 \tag{4-4}$$

For a_1 and a_2 as the radii of curvature of the liquid layer, Laplace's formaula may be used which gives the change in pressure due to surface tension effects.

$$P_c = -\sigma(1/a_2 - 1/a_1) = -\sigma(a_1 - a_2)/(a_1 a_2) \tag{4-5}$$

Substituting Eqs. (4-2) - (4-4) into (4-1) yields

$$\begin{aligned} F_c &= 2\pi a_1 \sigma + \pi a_1^2 \sigma(a_1 - a_2)/(a_1 a_2) \\ &= \pi a_1 \sigma(a_1 + a_2)/a_2 \end{aligned} \tag{4-6}$$

Using the radii of the particulates to express a_1 and a_2

$$a_1 = r(1 + \tan\alpha - \sec\alpha) \tag{4-7}$$

$$a_2 = r(\sec\alpha - 1) \tag{4-8}$$

If Eqs. (4-8) and (4-7) are substituted into Eq. (4-6), there is obtained

$$F_c = \frac{\pi\sigma r(1 + \tan\alpha - \sec\alpha)\tan\alpha}{(\sec\alpha - 1)}$$

(4-9)

$$= \frac{2\pi\sigma r}{1 + \tan(\alpha/2)}$$

If one of the surfaces is plane, the height of the fluid on the gap is twice as small, so

$$F_c = 4\pi\sigma r/(1 + \tan(\alpha/2))$$ (4-10)

For unwetted surfaces, F_c must be multiplied by the cosine of the wetting angle.

When capillary forces are present, the effect of any additional forces due to electrical pontentials may be neglected [11]. Thus the only additional force on a particulate helping it through the entrance zone is that due to capillary forces. When capillary forces are added to a single model spherical particulate on a plane mating-surface, the minimum coefficient of friction necessary to move a spherical particulate toward the interfacial zone is reduced.

To find the minimum coefficient of friction, μ, under conditions of capillarity, the effect of the ring of fluid acting on the model spherical particulate must be assessed as well as the increased normal force on the particulate. Figure 5 is a freebody of the forces acting on the particulate. The moments may again be summed about any point and the sum equated to zero as was done before to determine the value of μ min, the coefficient of friction between particulate and mating surface corresponding to a state of incipient rolling motion. The forces are as shown in Figure 5 and the moments about the points where the sphere contacts the elastomer will be considered.

$$F_N, c = F_N + F_c = F_A\cos\theta + F_c$$ (4-11)
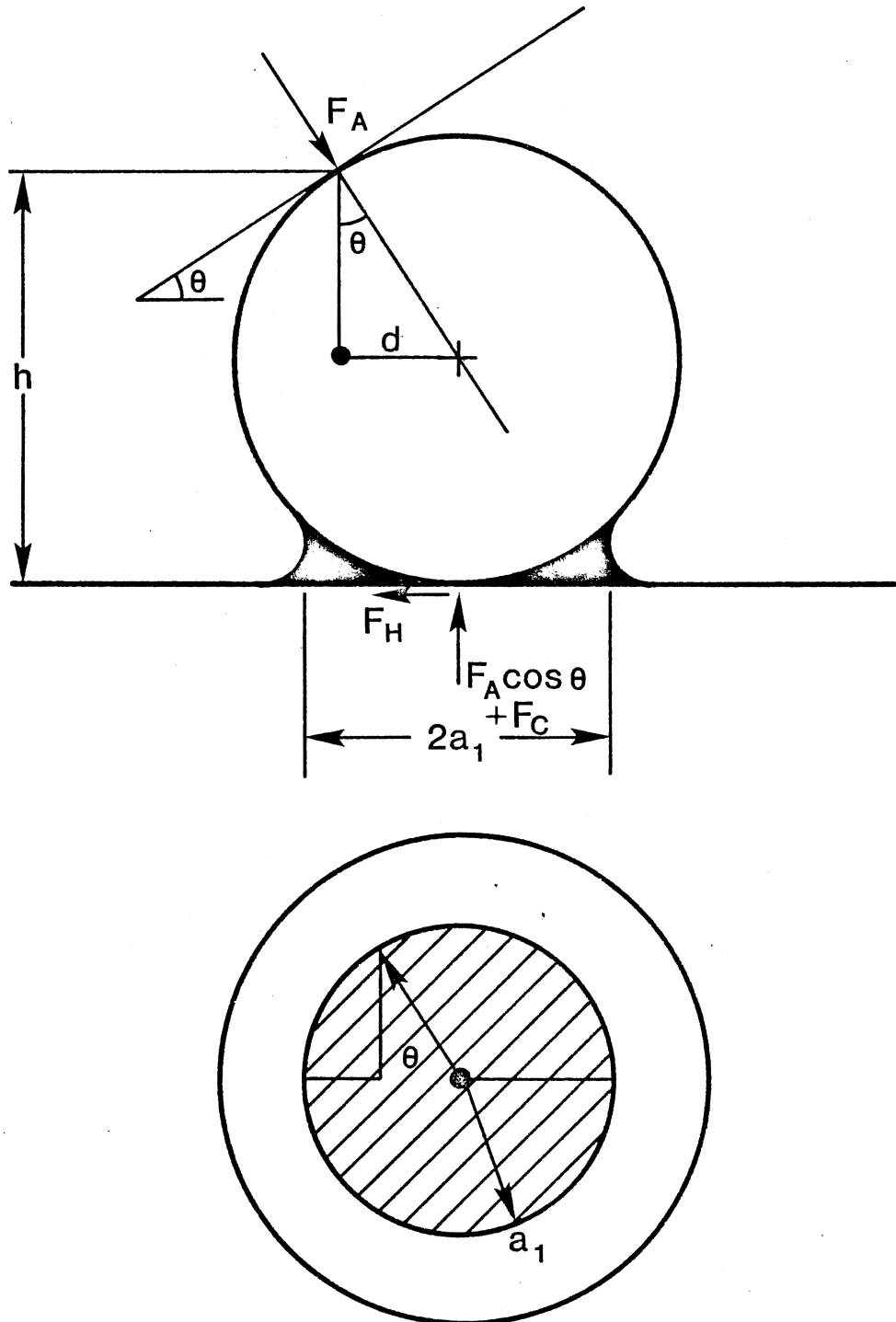
Figure 5. The Forces on a Spherical Particulate in the Entrance
Zone in the Presence of Capillarity.

where $F_{N,c}$ = The normal force between the particulate and the plane
when capillarilty effects are present.

The ring of fluid itself due to the presence of capillarity has
no effect on a single spherical particulate as can be deduced from
Figure 5.   As can be seen in the figure, the forces due to capillarity,
both the downward pull on the particulate by the menisus and the down-
ward force due to negative gage pressure are uniformly distributed
about the particulate. In fact, the sum of all these forces is
resisted by an equal and opposite upward force of the plane surface.
It is known from elementry mechanics, and the result can be easily
proved by use of the calculus, that uniformly distributed forces
may be represented by a single force of magnitude equal to the sum
of the distributed forces whose point of action is the centroid of
the uniform distribution and that this single force is suitable for
moment calculations. This centroid is the point where the sphere con-
tacts the plane and thus two equal but oppositely directed forces are
canceled at this point resulting in no change in moment about any point
due to the ring of fluid itself which is present with capillarity.

It is seen tht the increase in tangential force at the point where
the particulate contacts the plane, due to the increased normal force,
will result in a reduction in the necessary coefficient of particulate-
mating surface friction needed to initiate movement of the particulate
along the entrance zone. Since $d/H = F_H/F_N = \mu min$ and since $F_H/F_{N,c} = \mu_c$, the minimum coefficient of friction is reduced by capillarity to

$$(d/H)(F_N/F_{N,c}) = (F_H/F_N)(F_N/F_{N,c}) =$$

$$\mu_{min}(F_N/F_{N,c}) = \mu_c$$

(4-12)

where μ_c = the necessary coefficient of friction when capillarity

is present.

The maximum F_N, c occurs when the thickness of the interspersed fluid between particulate and mating surface goes to zero, as shown by Eq. (4-10). Thus the minimum coefficient of friction possible will occur for this condition. The value μ_c becomes, from Eqs. (4-12), (4-11), (3-11) and (3-1)

$$\mu_c = (d/h)[F_A\cos\theta/(F_A\cos\theta + 4\pi\sigma r/(1 + \tan\alpha/2))] \qquad (4-13)$$

Since F_A is an infinitisimal force at the initial point of particulate elastomer contact, Eq. (4-13) suggests that every particle will at least start its journey along the entrance zone no matter how small the actual particulate-mating-surface friction coefficient as long as the particulate is not completely immersed. Depending on the material properties of the elastomer and its changing slope in the entrance zone, F_A may increase due to elastic interference to the point where μ_c exceeds the available μ and the particle could then no longer continue moving along the entrance zone. This is different from the previous analysis in Chapter III where, when capillarity effects are not present, if the particulate is able to ever start moving along the entrance zone, it will continue to move along the entrance zone.

CHAPTER V

PARTICULATE SHEETS: THEIR EFFECT ON

PARTICULATLATES IN THE ENTRANCE ZONE

In Figure 6, the instantaneous center of rotation of a model spherical particulate is shown. It always lies along an axis normal to the mating surface which passes through the center of the sphere. Point B moves at some speed up to a maximum value equal to that of the mating surface. This gives an angular velocity of

$$\ell/V_B = \omega \qquad (5\text{-}1)$$

where ℓ = distance from the point of particulate contact with the

mating surface to the instant center;

V_B = velocity of point B;

ω = angular velocity of the particulate

which results in a velocity of point A of

$$V_A = \omega(\ell - r) \qquad (5\text{-}2)$$

where V_A = velocity of point A

r = particulate radius

Thus point A moves more slowly than point B by the ratio of

$$V_A/V_B = \omega(\ell - r)/\omega\ell = 1 - r/\ell \qquad (5\text{-}3)$$

It can be seen by Eq. (5-3) that as the slope of the elastomer in contact with the particulate decreases, the ratio of the velocity of point A to that of point B approaches one-half and that it is only as the contact slope of the elastomer approaches 90° that point C

22
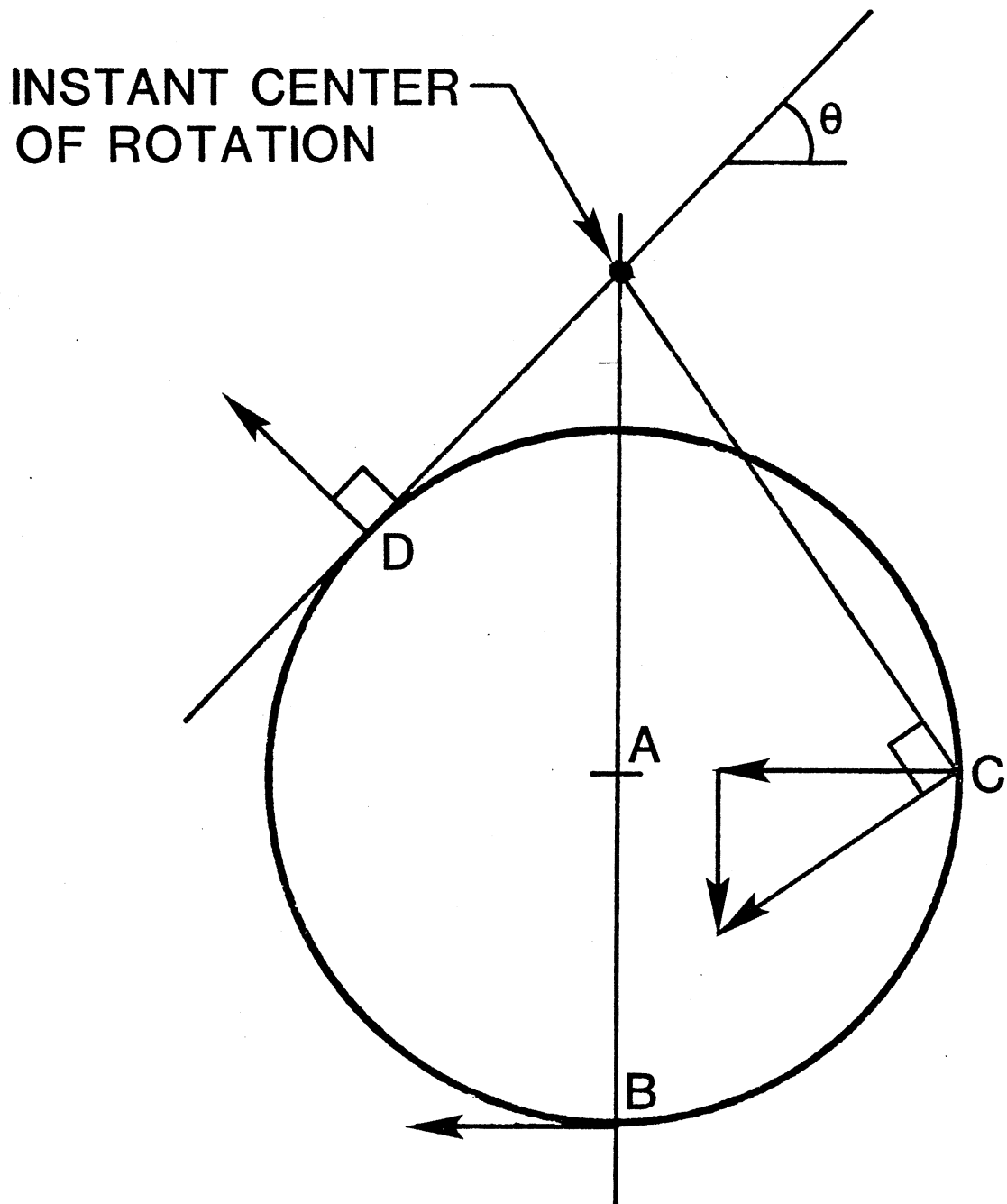
Figure 6. The Instantaneous Center of Rotation of a Model Spherical Particulate.

moves as fast as point A and B and that point C moves in the same direction as point A and B.

In Figure 7, a series of model spherical particulates of the same size are shown touching each other. This figure represents a particulate sheet, the first or leading particle of which is in contact with the elastomer. The particulates not in contact with the elastomer will move with the speed of the mating surface if not restrained in any way. As it is, the lead particulate sheet is impressing itself on the lead particulate. There is thus an additional force from the particulate sheet on the lead particle and the additional force may be sufficient to propel an otherwise immovable particulate toward the interfacial zone.

As seen in Figure 7, if the lead particulate is moving at maximum speed, it still is not moving as fast as the speed of the mating surface and hence for all conditions, the mating surface is slipping by the particulates in the particulate sheet even if it is not slipping by the lead particulate. Thus the maximum tangential force of the mating surface is always acting on the particulate sheet.

Since the particulates are in intimate contact with each other, there is an additional restraining moment on the lead particulate by the particulate sheet. Figure 8 shows a three particulate sheet with the lead particulate in contact with the elastomer. The end particulate is held by capillarity to the mating surface which causes it to produce a horizontal force on the middle particulate of

$$F_T = \mu F_c \qquad \qquad (5\text{-}4)$$

where F_T = force transferred by one particulate to another due to capillarity.
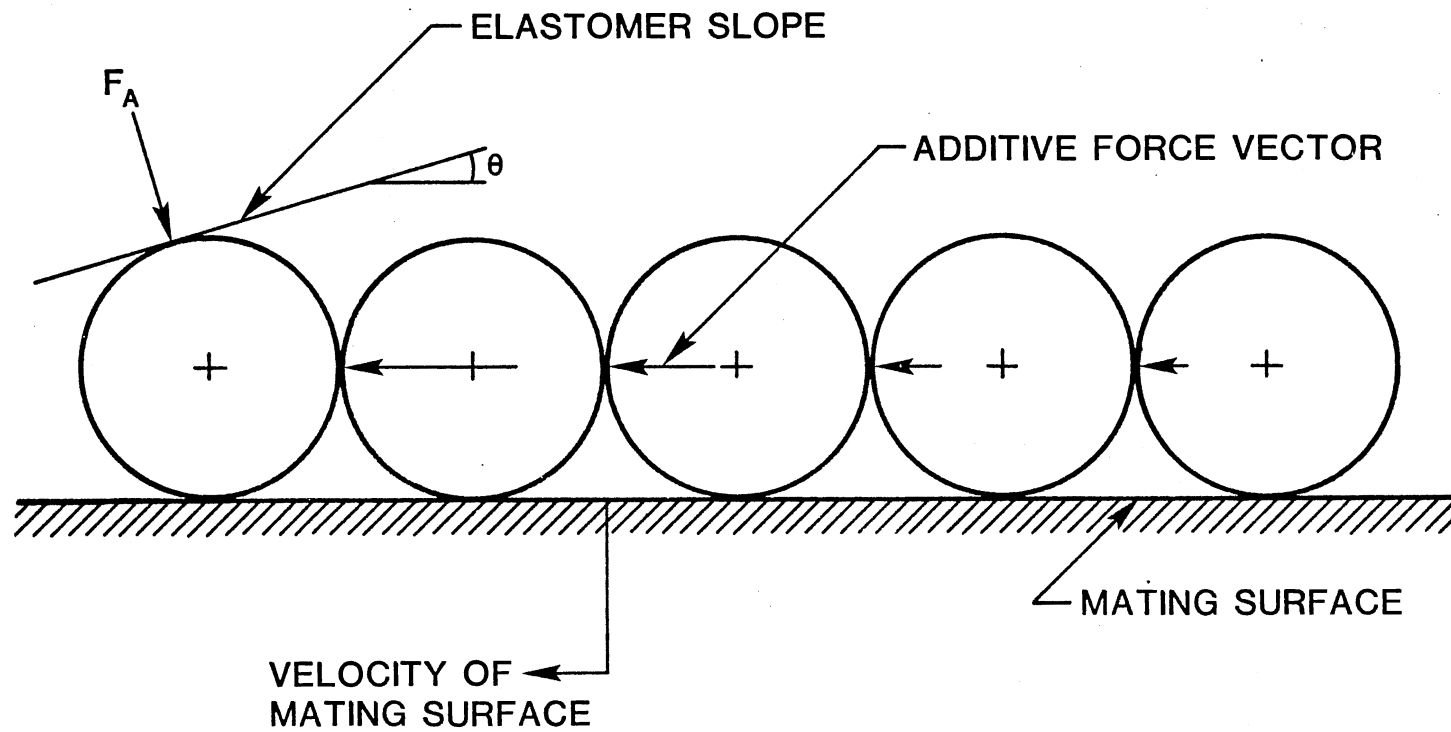
Figure 7. Additive Force on the Lead Particle due to a Particulate Sheet.
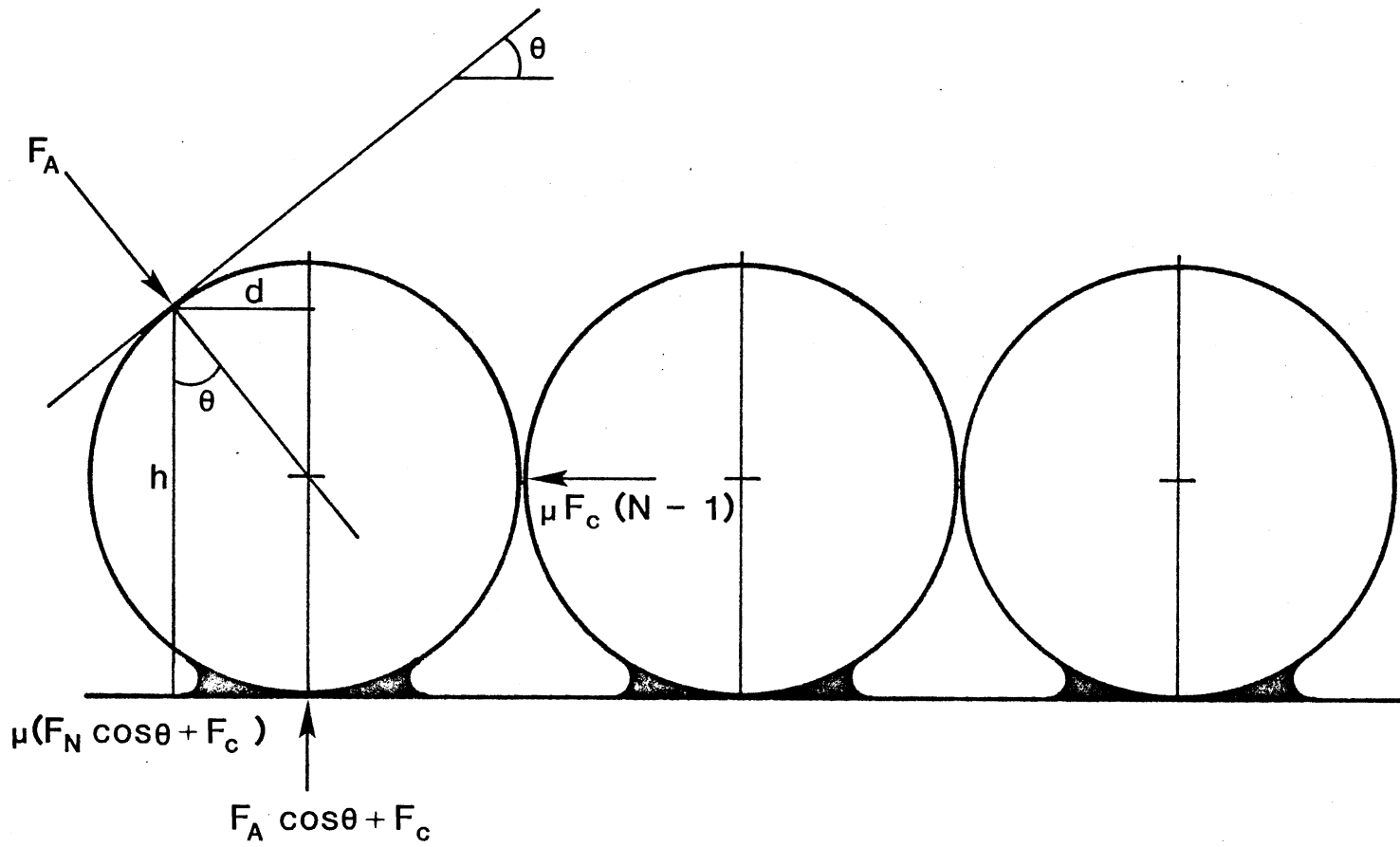
Figure 8. The Force on the Lead Particulate due to a Particulate Sheet.

The middle particulate transfers the force of the end particulate against the lead particulate and produces its own force against the lead particulate of equal strength to that produced by the end particulate. Thus the additional force on the lead particulate of a particulate sheet, all of the same particulate size, is

$$F = \mu F_c (N - 1) \tag{5-5}$$

where N = the number of particulates in the particulate sheet.

To find μmin, the minimum coefficient of friction between particulate and mating surface, assume a moment balance on the lead particulate such that in the rest of the particulate sheet, none of the particulates is rotating and that the moments on the lead particulate are in equilibrium.

$$0 = \Sigma M = - dF_A \cos\theta + \mu(F_A \cos\theta + F_c)h - $$
$$\mu_p \mu F_c (N - 1)(r + d) + \mu F_c (N - 1)(h - r) \tag{5-6}$$

which leads to

$$\mu_{min} = F_A \cos\theta \sin\theta / \left\{ F_A \cos\theta (1 + \cos\theta) \right.$$
$$+ F_c [N(\cos\theta - \mu_p(1 + \sin\theta)) + 1 + \mu_p \tag{5-7}$$
$$\left. (1 + \sin\theta)] \right\}$$

where μ_p = coefficient of friction between particulates.

Equation (5-7) shows that as the number of particulates, N, increases, μmin will either increase or decrease depending on the slope of the elastomer and the value of μ_p. Eq. (5-7) reduces to Eq. (4-13) when N = 1, as it should.

It was shown earlier that the translational velocity of all the particulates in the particulate sheet are less than that of the mating-

surface velocity due to the interaction of the lead particulate with the elastomer. In the previous derivation of the effect of particulate sheets on the reduction of the coefficient of friction necessary to move the lead particulate toward the interfacial zone, it was assumed that the particulates were not rotating. This assumption requires that the summation of the moments on each particulate be zero. If it is assumed that the particulates do not rotate, the following analysis applies. Figure 9 shows several particulates of a certain particulate sheet, all the particulates being spherical and of the same size. On any particulate between the lead and end particulates, the sum of all the moments acting when referenced to the center of the sphere is

$$\Sigma M = r[F_c\mu - (F_c\mu)(N - n + 1)\mu_p - (F_c\mu)(N - n)\mu_p] \qquad (5-8)$$

where F_c = normal force between the particulate and the mating surface due to capillarity;

  μ = coefficient of friction between the particulate and the mating surface;

  μ_p = coefficient of friction between two particulates;

  n = the particulate number location where the lead particulate is the number one particulate;

  N = number of particulates in the particulate sheet;

  r = radius of the spherical particulate.

If the particulate is to remain non-rotative, Eq. (5-8) must equal zero. Setting Eq. (5-8) equal to zero results in

$$\mu_p \geq 1/[2(N - n + .5)] \qquad (5-9)$$

Thus for the particulate next to the end particulate in Figure 9
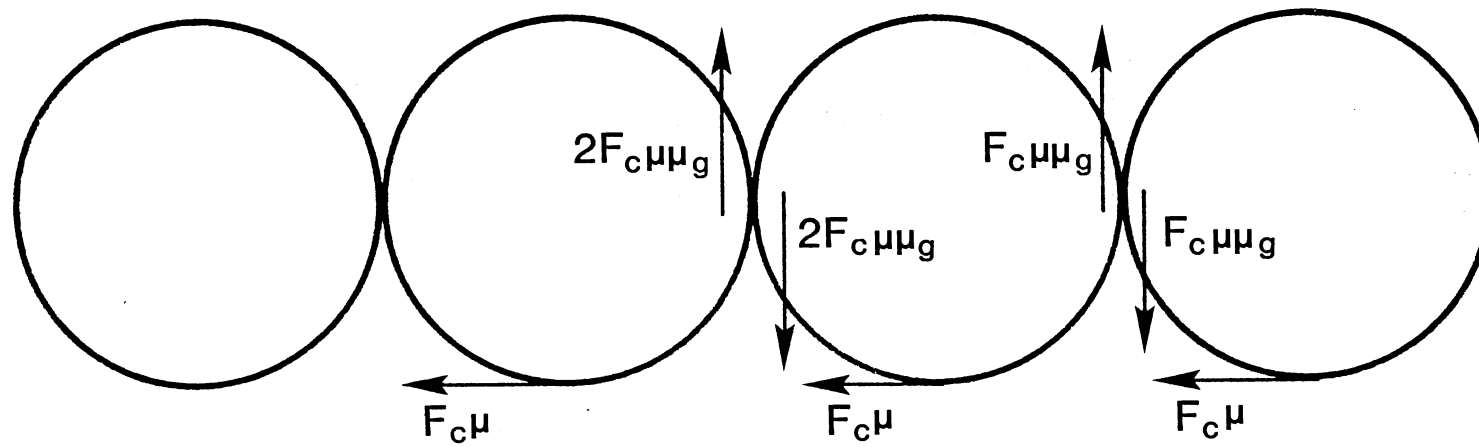
Figure 9. The Restraining Moments on Particles of a Particulate Sheet.

$$\mu_p \geq 1/[2(4 - 3 + .5)] = 1/3 \tag{5-10}$$

Thus for the particulate next to the end particulate, if the coefficient of friction between particulates is greater than or equal to 1/3 it will not rotate. For a particulate two particulates from the end, the coefficient of friction between particulates must be greater than or equal to 1/5. It can be seen that for a finite number of particulates, the necessary coefficient of friction between particulates to ensure no rotation decreases as the lead particulate is approached. For a partiuclate near the end, the coefficient is easily attained by many materials. Thus, as long as the end particulate a can exert a force equal to its coefficient of friction with the mating surface times the capillary force aginst the particulate next to it, the particulate sheet will be a rigid group of particulates all enforcing movement of the lead particulate toward the interfacial zone.

For the end particulate to remain stationary, either the coefficient of friction between particulates must be equal to or greater than 1.0 or capillarity effects between particulates must increase the normal force between the end particulate and its neighbor sufficiently to produce and equal and opposite moment to that produced by the particulate-mating-surface interface. Such a situation is shown in Figure 10. For a given coefficient of friction between particulates which is less than 1.0, the additional force due to capillarity needed to resist rotation is given by

$$\mu_p(F_{cp} + F_c\mu)r = (F_c\mu)r \tag{5-11}$$

which becomes

$$F_c\mu(1/\mu_p - 1) = F_{cp}$$

ADDITIONAL CAPILLARITY FORCE
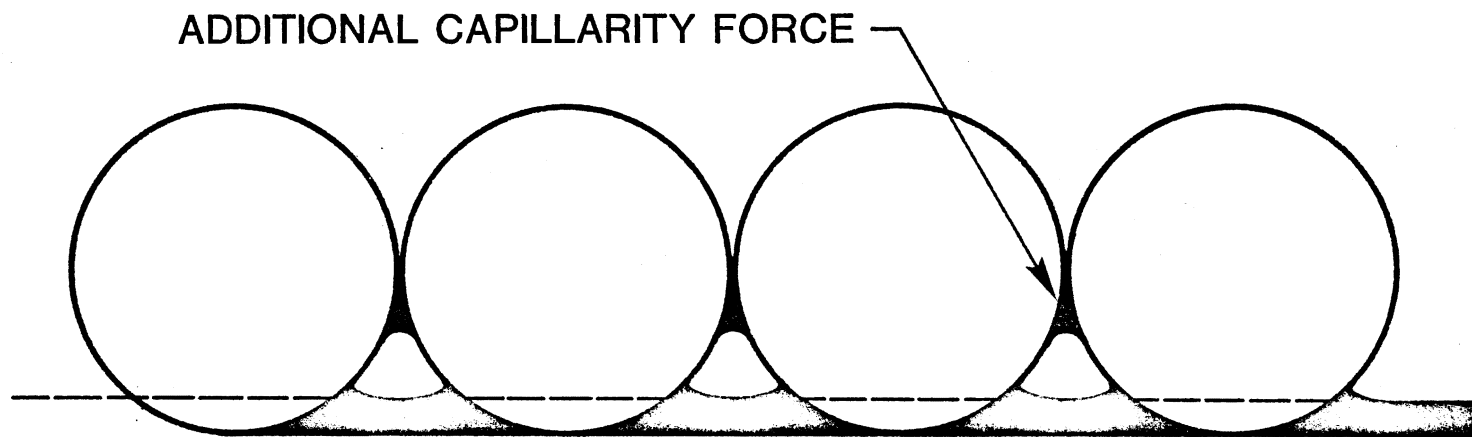
Figure 10. Additional Capillary Force on the End Particle of a Particulate
            Sheet.

where F_{cp} = the normal capillarity force between two particulates.
If it is assumed that μ and μ_p are less than one (which is true for
glass particles and metal mating surfaces) and that μ_p is > .5 (which
is true for glass) then F_{cp} is less than F_c. Such an additional force
is very possible.

   If the coefficient of friction between particulates is less than
one and capillarity effects are not present to increase the normal
particulate to particulate force, then the end particulate will
rotationally accelerate until it's perpheral speed matches that of
the mating surface. When this happens, the transmitted force must
drop to zero as otherwise the particulate will continue to accelerate
which it cannot do once its peripheral speed matches that of the mating
surface. The time it takes to do this should be almost instantaneous
considering its small size and corresponding small moment of inertia.
This effect would transfer rapidly through the sheet reducing the
effect of the sheet on the chances for a particulate to pass through
the entrance zone.

CHAPTER VI

ENERGY LOSSES: RESISTANCE OF ELASTOMERS
TO ROLLING PARTICLES

The concept of rolling friction has changed over the years with
the first recorded observations being by Leonardo da Vinci [12].
Coulomb [12] showed tht rolling friction is proportional to load
and inversely proportional to the diameter of a cylinder. Osborne
Reynold's [12] experimental work agreed with that of Coulamb.
Reynold's [12] claimed that rolling resistance is due to the same
causes as ordinary sliding friction.

Tomlinson [12] believed that rolling resistance is due to
molecular adhesion. Heathcote [12] showed that for a sphere as
opposed to a cylinder, an important source of interfacial slip not
mentioned by Reynolds is the rolling of a sphere in a groove.
Different parts of the region of contact are at different distances
from the spherical axis of rotation. The sphere therefore measures
out different distances as it rolls producing differential slip
in the elliptical contact area.

Tabor [12] makes that observation that the major contributors to
a theory of rolling friction, Reynolds [12], Heathcote [12], Tomlinson
[12], all rely on some sort of surface interaction. He points out that
this notion does not explain the fact the lubricants do not affect the

magnitude of rolling resistance appreciably. Reynolds [12] knew that
lubricants did not affect rolling friction and tried to explain the
reasons for this by saying that the lubricant causes that degree of
micro-slip to decrease while it increases the area over which such
slip occurs and the result is that the friction remains practically
constant. Tabor [12] reconciles all these notions by showing that
although interfacial effects cause surface wear, they contribute
very little to observed rolling resistance. Tabor [12] shows, it
is now the accepted theory of rolling friction, that "the major part
of the resistance to rolling arises from elastic hysteresis losses
within the solids".

Many investigators, May [18], Halaunbrenner[19] and Flom [20]
to name a few, took up the theme of Tabor [12] and endeavored to
develop mathematical models for the elastic hysteresis losses of
rolling resistance. The usual pattern of most investigators is to
assume certain viscoelastic properties for the elastomer and then,
by knowing the rolling speed and roller geometry, determine the
strain history of the elastomer model and hence the stress history
of the same model. This stress history is imposed on the rolling
element which then determines the necessary additional external
forces to keep the element rolling at the specified speed while
impressed to the specified depth.

Tabor [12, 13, 14, 15] himself did not model elastomers as
viscoelastic solids. He instead used the notion of hysteresis
loss, which theory he developed with succeeding refinements over a
span of several years. Tabor [12] shows that for elastomers,
the hysteresis loss, (the percentage amount of energy not returned

to an indenter on with-drawing from an elastomer which was input to the elastomer during indentation) is constant for elastomers for constant rates of strain. Thus with this notion, Tabor [13] states that "the rolling friction, F, should be a constant fraction of θ, where θ is the work input to the elastomer.

Tabor [14] pressed half inch steel cylinders into elastomers, cyclicly loading and unloading the cylinders in about the sane time it took to roll the cylinders a distance equal to their arc length. He found that the percentage enrgy loss was dependent on strain rate but not on strain. The elastic input energy of a rolling cylinder was calculated and the hysteresis loss was determined and compared to measured rolling resistance. The result was that the calculated percentage of lost enery was about 1/2 of the actual loss.

Greenwood, Minshall, and Tabor [15] state that for cyclic uniform tension or torsion loading cycles performed at constant rates of deformation, the energy loss is normally assumed to be a constant fraction of the input enery. This fraction is known as the hysteresis loss factor. They point out that while rolling friction depends on load, ball diameter and elastic elastomer constants, as predicted by the hysteresis loss factor theory, the measured values of friction exceed the theoretical values by two or three times. They conclude from this that it is incorrcet to apply a hysteresis loss factor obtained from a simple deformation cycle to the more complex cycles which occur during rolling. For a simple compression deformation cycle an amount of energy, ε, is expended in deforming the elastomer. The percentage of this deformational energy which is lost during a cycle is α.

Now if during the rolling of a hard object over an elastomer
the elastic energy required to deform the elastomer per unit distance
of rolling is θ, the rolling resistance can be assumed to be

$$F = \alpha\theta \qquad (6\text{-}1)$$

where F = the rolling resistance.

How F depends on load and ball diameter, the material elastic con-
stants, and on α is correctly demonstrated by Eq. (6-2) but the
absolute magnitude of F is too small be a factor of 2 or 3. The
discrepenacy occurs because ε is not true criterion of elastic
hystereisi energy loss.

Greenwood, Minshall, and Tabor [15] showed that hysteresis
losses may occur even if the elastic strain energy at any point is
constant. For elastomers, Poisson's ratio is nearly 0.5 so that
only the shearing energy losses in the elastomer need be considered
since for incompressible elatomers no energy loss should occur with
hydrostatic stresses. By plotting the two shear stresses of a plane
element - which occur at 45° to one another - against one another,
a stress loop is formed.

The energy loss is proportional to the square of the length of
the loop. By summing the squares of the lengths of all loops at
each point over the whole volume of the elastomer, the energy lost
and hence the resistance can be found for rolling. Good results
were obtained by this method.

Other investigators do not follow Tabor's [16] approach. Indeed,
Tabor's [16] approach is valid for only very slow rolling speeds. Nor-
man [17] shows that as the viscoelastic loss tangent, tanδ, increases,
Tabor's [16] approach becomes more and more in error. The reason is
that Tabor [16] assumed a symmeriacl draping of the elastomer about

the roller for all rolling speeds while in reality, as $\tan\delta$ increases, the contact becomes asymmetrical with the elastomer loosing contact behind the roller earlier and earlier. This leads to additional rolling resistance.

All the researchers approaching rolling resistance from the viscoelastic point of view have limited their treatment to that of small deformations [17, 18, 19, 20, 21]. The reason for this is given by Halaunbrenner and Dubisz [19] in their excellent paper dealing with hard balls rolling on viscoelastic plates. In part two of their paper these two investigators state: "A set of problems concerning the rolling of rigid ball on a viscoelastic base comprises the following items: Rolling resistance, size and shape of the contact area and deformation of the base surface in the vicinity of the contact area as functions of velocity, normal load, and machanical properties of the base. These have not as yet been solved strictly within the elasticity theory. The main diffiuclty lies in the lack of knowledge of the shape of the contact surface." This lack of Knowledge of the shape of the contact surface severely limits the development of mathematical models describing accurately the rolling resistance of rollers impressed with more than a few percent of strain into the base elastomer.

Elastomers do not have a linear stress strain curve [22]. Thus the classical equations of elasticity, which assume Hookes law is operative (stress vs strain is linear), do not apply to rubber elasticity. It would be alright however to apply them about an operating point where the stains are sufficiently low to be able to

assume a linear stress versus strain relationship at the point.

Elastomers will experience viscoelastic behavior under the action of applied forces and displacements. When strained to a certain extension and held in this position, elastomers will experience a relaxation in stress. If stressed to a certain level, elastomers will creep, increasing in strain for no further increase in stress. The behavior of the material is determined by its stress history as well as its present stress.

A principle put forth by Boltzmann [22] in 1874 makes it possible to predict elastomer behavior for an arbitrarily varying stress with time if the material behavior under constant stress is known. The principle is: the total deformation at any time due to a time varying loading condition is the sum of the deformations which would have been produced by each separate load; the removal of a load being regarded as an application of a negative load. For this principle to apply, the deformations (both time-dependent and instanteous) must be linearly proportional to the stresses. It can only be used then when the strains are small.

Materials may be represented by springs and dashpots as shown in Figure 11 and it is possible to represent their behavior by using a great number of such devices, each spring-dashpot system having its own relaxation time. Two spring-dashpot systems are shown in Figure 12. The relaxation time (sometimes called the retardation time)is defined as

$$\tau = \eta/G \qquad (6\text{-}2)$$

To use such a model implies that the stress obey Boltzmann's super-postion principle. If a distribution of relaxation times can be
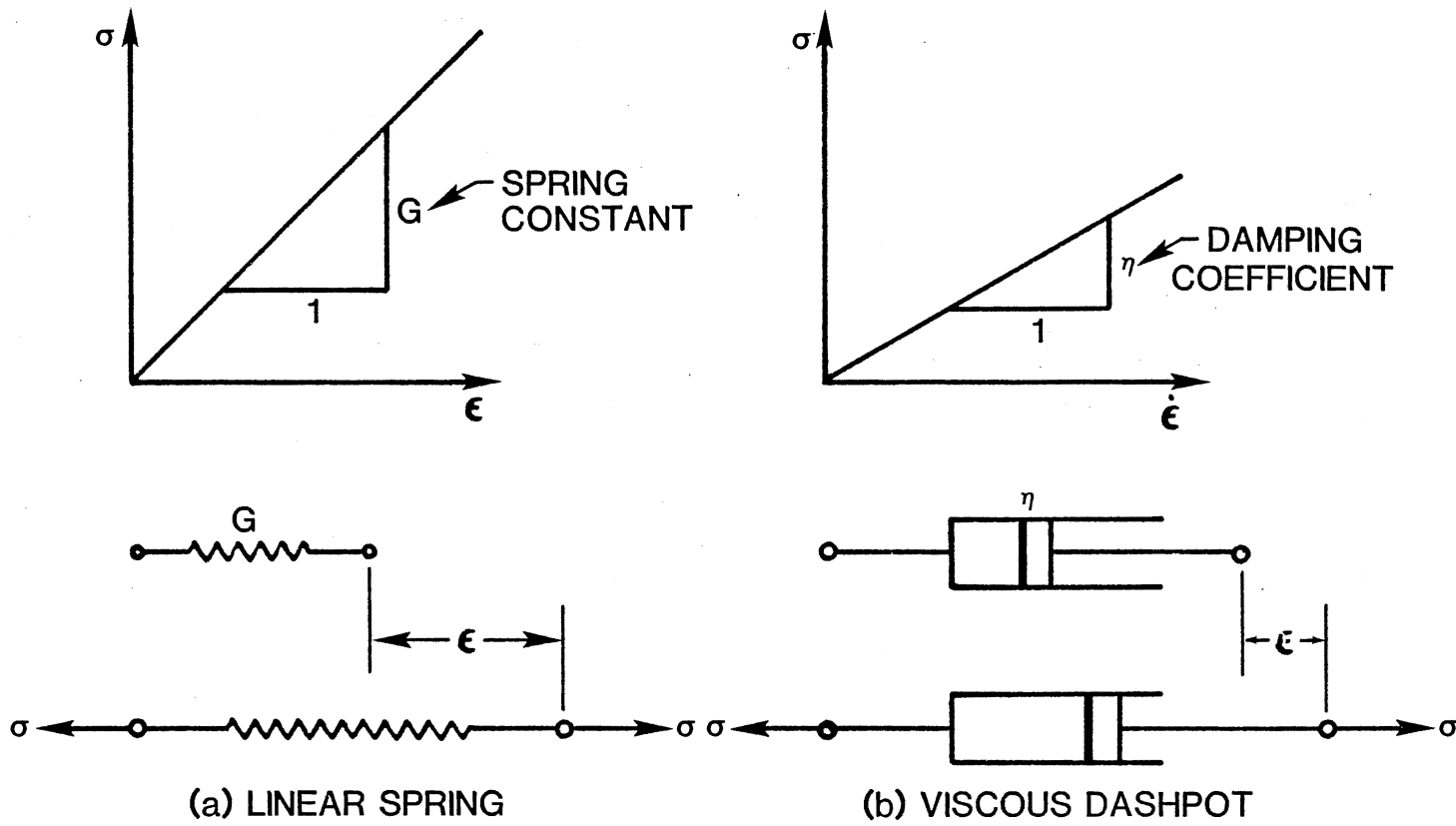
Figure 11. Elements Used in the Representation of Viscoelastic Material Properties.
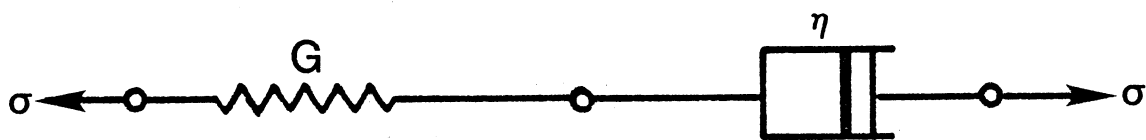
(a) MAXWELL
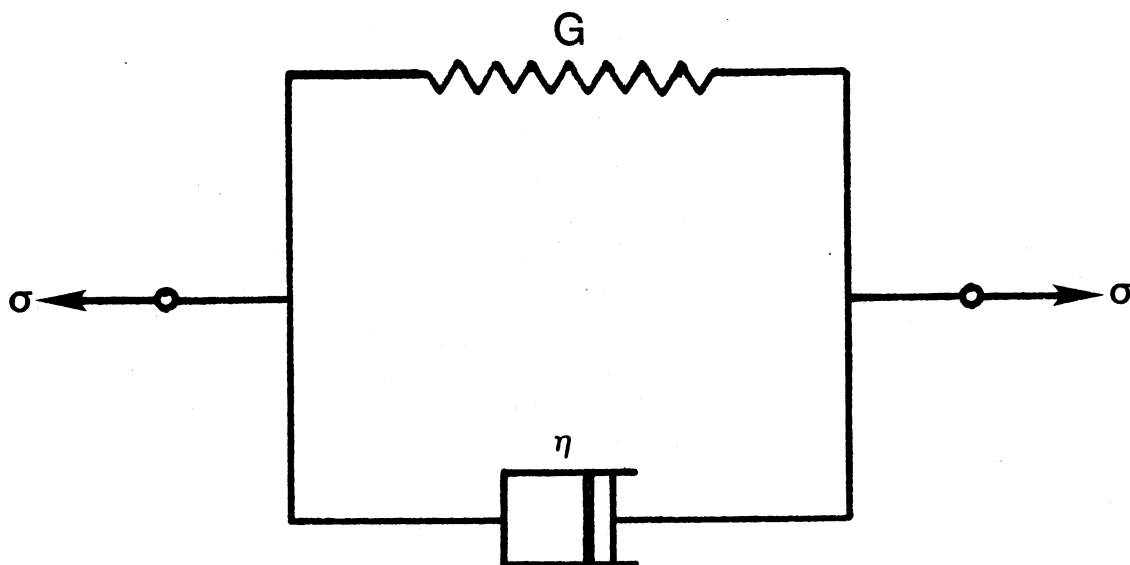
(b) VOIGT – KELVIN

Figure 12.   Two Commonly Used Spring Dashpot Systems Used to Represent Viscoelastic Material Behavior.

found which reproduces the elastomers behavior for a given strain history, its behavior under any other history of strain can be referred back to the same system of springs and dashpots.

Resilience of elastomers is a property which shows the ability of the elastomer to store and return an amount of energy in a rapid deformation. Two parameters, time and temperature, determine a given elastomer resilience.

While models of springs and dashpots are used to show elastomer behavior, it must always be remembered that they are empirical in nature, they do not imply that such things exist in the elastomer [21, 22]. They should be looked at as aids to the description and interpretation of complex visco-elastic behavior.

Elastomers do not correspond in their behavior to Maxwell or Kelvin models, use must be made of multiple-element systems. To represent complex types of viscoelastic behavior requires use of a large number of relaxation times (spring-dashpots). Whether use is made of a number of Maxwell elements in parallel or a number of Voight-Kelvin elements in series does not matter. The two different approaches can be shown to be mathematically equivalent if one degenerate element is included in each model (the element having either a spring or a dashpot missing). Figure 13 shows a visco-elastic model made up of an infinite number of Maxwell system elements each with its own relaxation time. By removing one spring and one dashpot, but both not from the same system, will produce a model with an infinite spectrum of relaxation times. This is taken from $\tau = 0$ to $\tau = \infty$.

A material can be represented by the concept of a distribution

of relaxation times if experimental evidence or a knowledge of its structure indicates that this is so. It is not a purely mathematical problem. The distribution function, if it exists, may be different for different types of strain, that is, if the deformations are extensional or shearing. It must be assumed that the material has a linear stress strain curve for an instantaneous strain.

If stress depends on both strain and strain rate and/or also higher derivatives of strain, then these deviations from classical elastic material obeying Hooke's law -- stress proportional to strain-- are classified as viscoelastic. Linear viscoelasticity occurs when the ratio of stress to strain depends only on time [21]. Sliding and frictional processes with elastomers are seen as viscoelastic effects mainly because of the WLF (Williams, Landel, Ferry) transform correlation. This transformation allows elastomer frictional data obtained at various temperatures to be presented on a single master curve. The WLF transform is characteristic of viscoelastic materials and its successful application to frictional data can be taken as indicating the frictional process is a viscoelastic process.

Investigators using the viscoelastic approach to rolling resistance use one or more of three approaches. May, Morris and Atack [18], Flom and Bueche [20], and Moore [21] model the elastomer base upon which a hard object moves by a system of independent vertical columns where each column is made up a generalized Maxwell model as shown in Figure 13 or some simplification of this model such as a finite number of relaxation times. The roller is moved over the surface at a specified depth. The elastomer is assumed to conform to the front half of the roller. The elastomer on the back side of
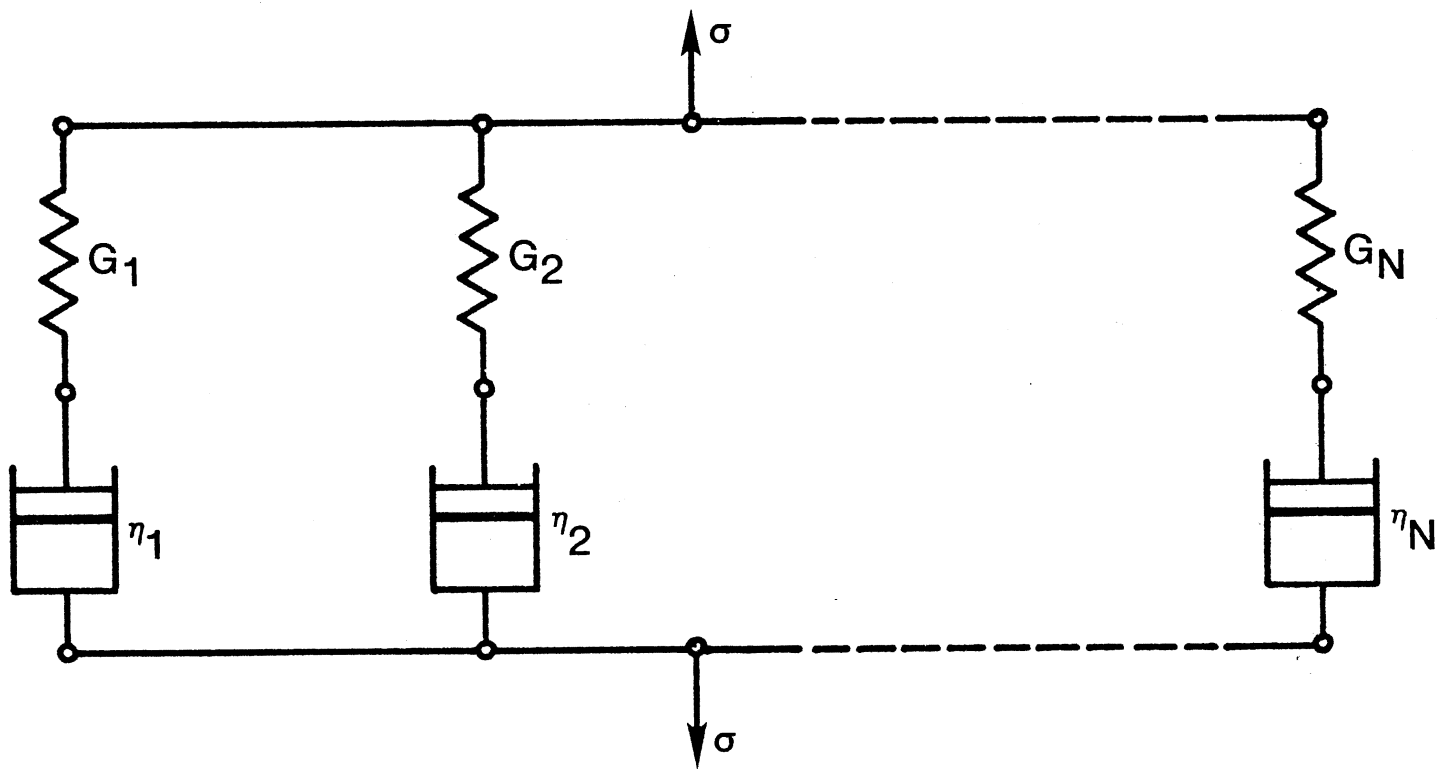
Figure 13. Viscoelastic Model Incorporating an Infinite Spectrum of Relaxation Times.

the roller relinquishes contact with the roller at a point where the stress is calculated to be zero. This asymmetry leads to a greater rolling resistance than is predicted by Tabor's [16] approach for the usual range of rolling speeds. By knowing the deformation history, the Boltzmann super position principle is applied to determine the stress history which is used in determining the rolling friction.

Norman [17] and Moore [21], in addition to the approach described above, used a slightly different approach where the tangen modulus of viscoelasticity is used. The tangent modulus or loss tangent is given by

$$\tan\delta = \frac{\omega\eta}{E'} \tag{6-3}$$

where $\tan\delta$ = loss tangent;

ω = circular frequency;

η = effective elastomer viscosity;

E' = dynamic Young's modulus (maximum steady state stress over the maximum steady state strain).

For rollers moving about on viscoelastic planes, the plane experiences deformation only once by the roller and so it is not strictly correct to speak of a circular deformation frequency. To overcome this difficulty, Moore [21] uses the reciprocal of the time it takes for the plane to be maximally deformed by the roller after making initial contact with it. Norman [17] uses the same analysis as Moore [21] except that he approximates the viscoelastiv plane deformation by a half sine wave. This results in Norman [17] using an angular frequency of one-half that of Moore [21]. The equation derived by Moore [21] and Norman [17] for the coefficient of the rolling friction

differ from each other in the value of certain constants but not in form.

May, Morris, and Atack [18], in addition to using their independent column approach, follow the theory of Pao [23] and derive the "exact" viscoelastic solution to their problem. The approach used is called the correspondence principle [24]. The general method as outline by Pao [23].

> The method of solution consists essentially of obtaining the Laplace transform of the elastic solution, replacing the shear modulus of the elastic case in the transformed expression with a viscoelastic function and obtaining the inverse transform of the altered expression. If the resulting expression satisfied the boundary and initial conditions of the physical situation, it is the unique viscoelastic solution to the problem considered (p. 1083).

This approach leads to more accurate results because the shear stresses are no longer neglected. For small deformations where elastic theory may be employed, the exact method produces curves very similar in shape to those produced by applying approximate methods,i.e., the independent column approach. The magnitudes are different since using approximate methods requires consideration of elastomer thickness whereas use of the exact methods does not.

As already stated, all the approaches assume small deformations in the analysis because large deformations have not as yet been solved strictly within elasticity theory. Thus only a small portion of the entrance zone may be modeled with accepted theory. The rest of the entrance zone and the interfacial zone, for particles that are large compared with the fluid film thickness, may not be so modeled and still have results which correspond closely with reality. Still, it is desirable to get some feeling for how defferent elastomers resist to a greater or lesser extent the trans-

port of particulates through the interfacial zone.

In order to arrive at some prediction of elastomer impedance to rolling, the following assumptions will be made:

1) The particulates are rigid cylinders.

2) The elastomer base is represented by a system of independent vertical columns.

3) Elastomer and particulate inertia will be ignored.

4) Adhesion and other superficial interactions are considered small enough to neglect.

This analysis will closely follow that of May, Morris, and Atack [18]. They derive relationships for the interaction of a cylinder with an elastomer base. The use of a modified form of the standard linear solid model will be used in this analysis. One purpose of this analysis is to show how rolling resistance depends on the parameters of elastomer moduli and the relaxation time. The main purpose of this analysis is to show the effect which a gross contact pressure has on rolling resistance. This constitutes an important original contribution to the theory of rolling resistance and is directly applicable to the problem with which this thesis is concerned.

Figure 14 shows a cylinder impressed into a viscoelastic base to a specified depth. Now

$$x^2 = 2r(z_0 - z) - (z_0 - z)^2 \qquad (6\text{-}4)$$

where: Z_0 = depth of penetration;

r = radius of the cylinder;

Z = depth of material compression at point $p(x)$.

If the cylinder moves at a velocity v, then
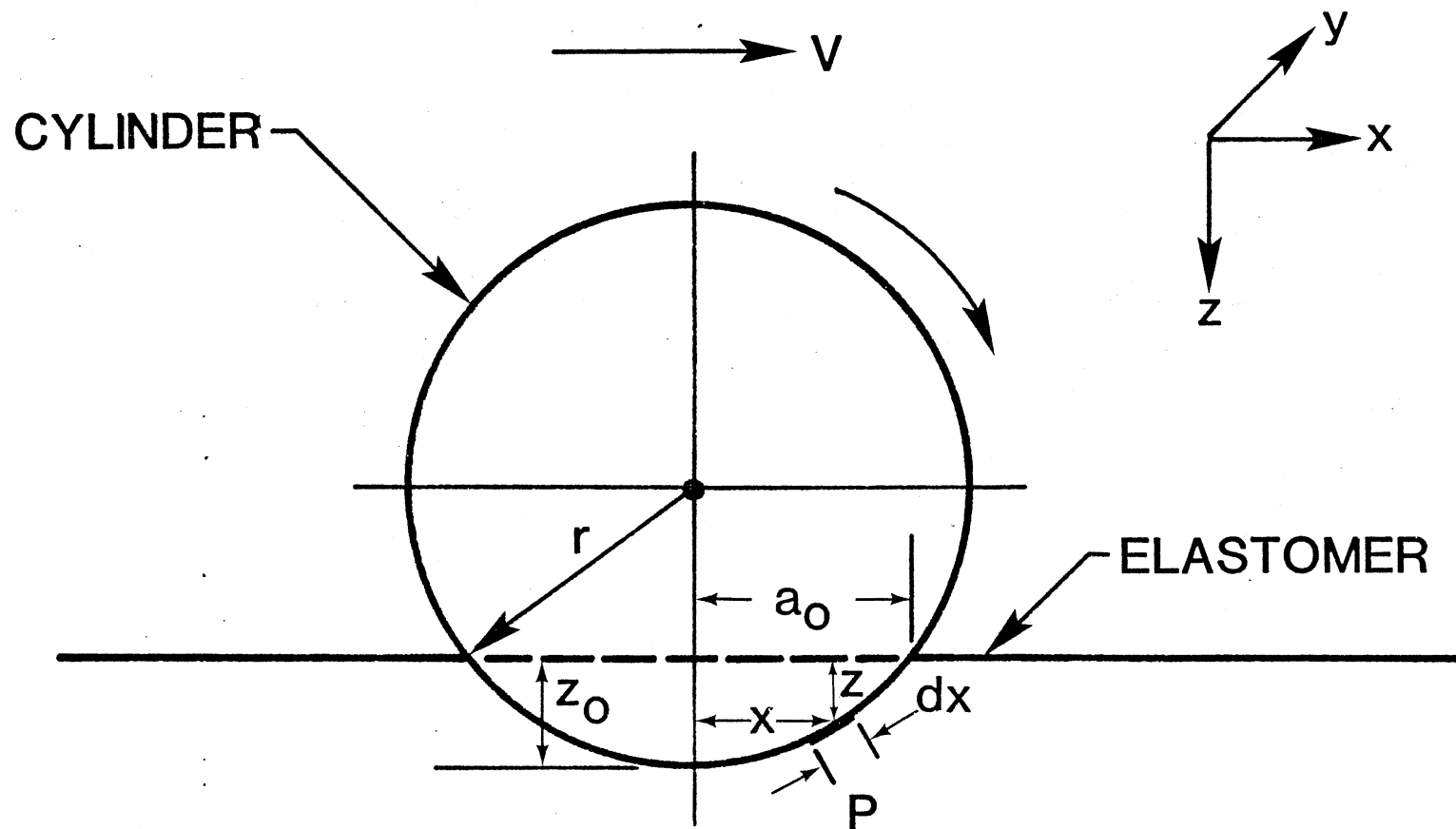
Figure 14.   Schematic of a Spherical Particulate Pressed into a Viscoelastic Base.

$$a_o - x = vt \qquad (6\text{-}5)$$

where t is time during which the material at point p has been in

compression. It is apparent that

$$a_o{}^2 = 2rZ_o - Z_o{}^2 \qquad (6\text{-}6)$$

Neglecting terms containing the square of the cylinder penetration

Z_o, the compression as a function of time is found by substituting

Eq. (6-5) into Eq. (6-4) to eliminate x and applying to this

Eq. (6-6). The result is

$$Z(t) = (v/2r)(2a_o t - vt^2) \qquad (6\text{-}7)$$

where Z(t) now represents the strain history of the elastomeric

viscoelastic base. Now allowing ℓ to be thickness of the base

material, the stress at point p after time t may be deduced by

applying Boltzmann's superposition principle.

$$\ell\sigma(t) = \int_0^t \phi\,(t - \theta)\,\frac{dZ(\theta)}{d\theta}\,d\theta + \ell P_c \qquad (6\text{-}8)$$

where $\sigma(t)$ = the stress at point p as a function of time;

$\phi(t - \sigma)$ = the material relaxation function;

P_c = contact pressure at the point x=y=z=0 when no

particulate is present.

The stress history $\sigma(t)$ will be obtained for a modified standard

linear solid viscoelastic system used to model the elastomeric

viscoelastic base. This system is shown in Figure 15. The re-

laxation function of such a system is given by

$$\phi(t - \theta) = (E_1 + E_2\,\exp[\,- (t - \theta)/\tau])[U(t - \theta)] \qquad (6\text{-}9)$$

where E_1, E_2 = moduli of the material;

τ = the relaxation time;
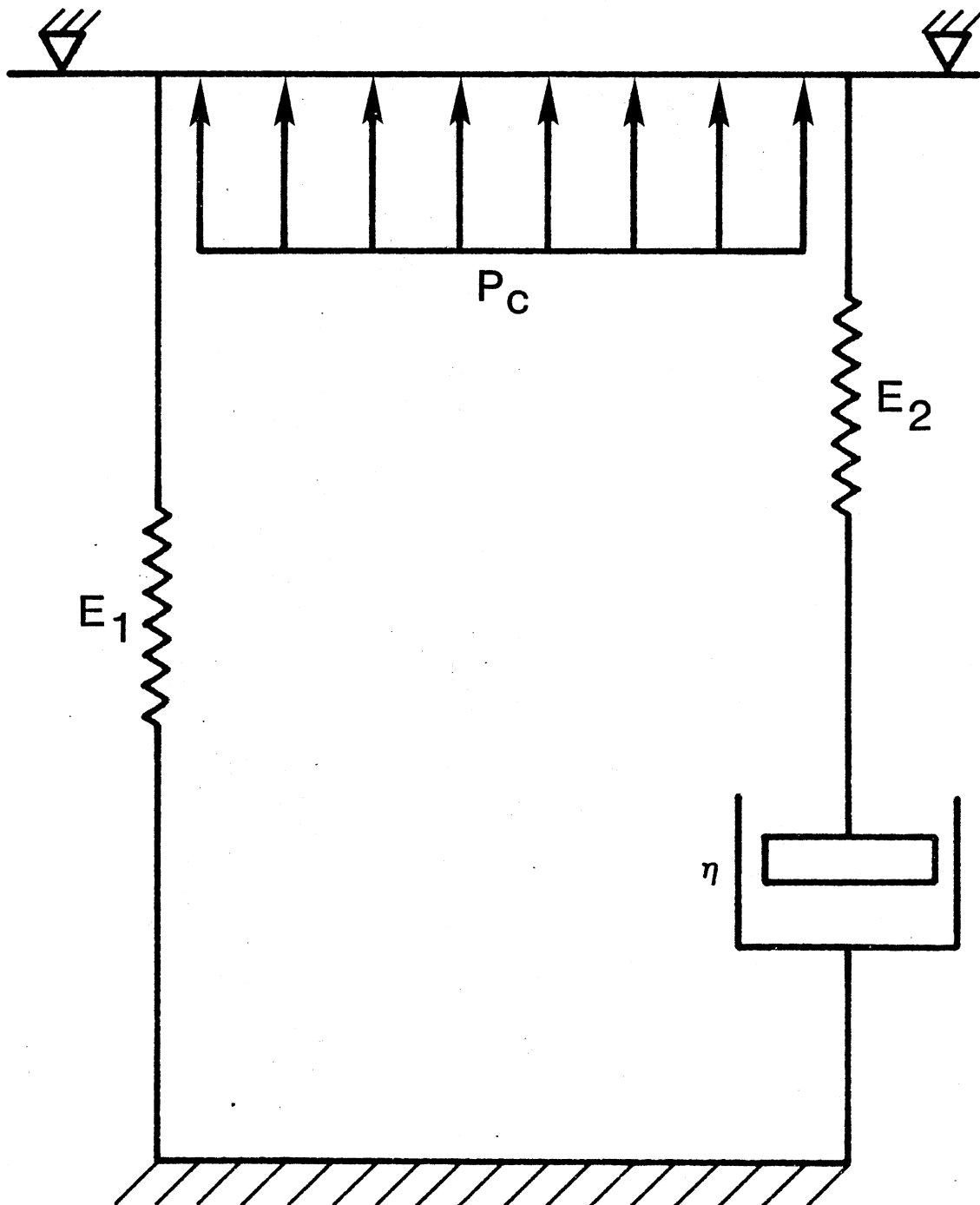
Figure 15. Modified Standard Linear Solid Viscoelastic System Model.

$[U(t - \theta)]$ = the Heaviside function,

Since the lower limit on the integral sign of Eq. (6-8) is zero, the relaxation function may be simiplified to

$$\phi(t - \theta) = E_1 + E_2 \exp[- (t - \theta)/\tau] \qquad (6\text{-}10)$$

and

$$dZ(\theta)/d\theta = (V/r)(a_0 - V\theta)., \qquad (6\text{-}11)$$

Substituting Eq. (6-10) and (6-11) into Eq. (6-8) yields

$$\ell\sigma(t) = V/r \int_0^t (E_1 + E_2 \exp[- (t - \theta)/\tau])$$

$$(a_0 - V\theta)d\theta + \ell P_c . \qquad (6\text{-}12)$$

This equation may easily be integrated by use of the following identity

$$\int \theta \exp[- (t - \theta)/\tau]d\theta = \tau(\theta - \tau)\exp[- (t - \theta)/\tau] + c . \qquad (6\text{-}13)$$

This results in

$$\sigma(t) = (VE_1/(2r\ell))(2a_0 t - vt^2) + (E_2 V\tau/$$

$$(r\ell))[(a_0 + V\tau)(1 - \exp[-t/\tau]) - Vt] \qquad (6\text{-}14)$$

$$+ P_c .,$$

Let k be defined as

$$k = \tau/T \qquad (6\text{-}15)$$

where T = time taken for the cylinder to move a distance equal to its semi-length of contact a_0.

The stress behind the cylinder where it leaves the material will be zero. This distance from the center line will be defined as X_0. X_0 depends on τ and can be discovered by setting $\sigma(t)$ equal to zero in Eq. (6-14). Taking $E_1 = 3E_2$ for comparison with May, Morris, and Atack[18] may be calculated in terms of k by setting $\sigma(t)$ in Eq. (6-14) equal to zero. This results in

$$\exp[- (1/K)((a_0-x_0)/a_0)]= ((a_0 - x_0)/a_0)[(6 -$$

$$2K - 3(a_0 - x_0)/a_0)/(2K(k + 1)) + Pr\ell/(KE_2 \qquad (6\text{-}16)$$

$$a_0(a_0 - x_0))] + 1$$

By letting $P = .25\ E_2$, $Z_0 = 1$, and knowing $a^2 = 2rZ_0$ Eq. (6-16) becomes

$$\exp[- (1/K)((a_0 - x_0)/a_0)] = ((a_0 - x_0)/a_0)[(6 -$$

$$2K - 3(a_0 - x_0)/a_0))/(2K(K + 1))] + .125/K + 1 \qquad (6\text{-}17)$$

which is the same equation as would result for a standard linear solid viscoelastic system but with the addition of the 0.125/k term which is due to the inclusion of the contact pressure in the visco-elastic system. This equation was solved numerically for various values of k and the results are shown graphically in Figure 16.

It is seen that for the specific value of $E_1 = 3E_2$ and for the values selected which resulted in Eq. (6-17), that X_0 is nearly equal to a_0 over all rolling speeds. The asymmetry of elastomer contact with the cylinder reaches a maximum when k is approximately equal to .5. It can also be observed that both the maximum asymmetry and the range of rolling speeds over which an appreciable asymmetry exists are less for the elastomeric viscoelastic system modified by the addition of the contact pressure P_c. Thus the intuitive notion that contact pressure should result in a more symmetrical draping of the elastomer about the particulate is shown to actually be so.

It is now desired to find what effect contact pressure has on the resistance by the elastomer to rolling. Intuitively, the addition of contact pressure should result in greater rolling

resistance but only at speeds where appreciable asymmetry of elasto-mer--cylinder contact occurs. This is seen to be true since rolling resistance causes an expenditure of energy which is dissipated by the dashpot of the viscoelastic system. Since the force across the dashpot is proportional to $\dot{Z}(t)$, the power dissipated is proportional to $\dot{Z}(t)$ squared. Thus when no appreciable asymmetry is present, intergration of the square of $\dot{Z}(t)$ with respect to time is the same whether or not additional contact pressure is present and hence the energy dissipated and the rolling resistance are the same. When asymmetry is present, the elastomer recovers to its original height after losing contact with the cylinder and during this recovery, all the potential energy in the springs and that due to contact pressure is dissipated through the dashpot. Thus when contact pressure is present, there is an additional potential energy source which must dissipate itself across the dashpot whenever asymmetry is present and thus contact pressure results in greater resistance by the elastomer to the rolling of a cylinder under conditions of asymmetry.

To derive an expression for the rolling resistance or friction, it is first necessary to sum the moments about the point $Z = Z_0$, $X = 0$ in Figure 14. From Eq. (6-14) and referring to Figure 14, there results

$$F(t) = (E_1 V/(2r\ell))(2a_0 t - vt^2)y_0 dx +$$

$$(E_2 v\tau/(r\ell))[(a_0 + v\tau)(1 - \exp[-t/\tau])- \qquad (6-18)$$

$$vt]y_0 dx + P_c y_0 dx$$

where $F(t)$ = the force on the strip d_x wide and y_0 long at point p
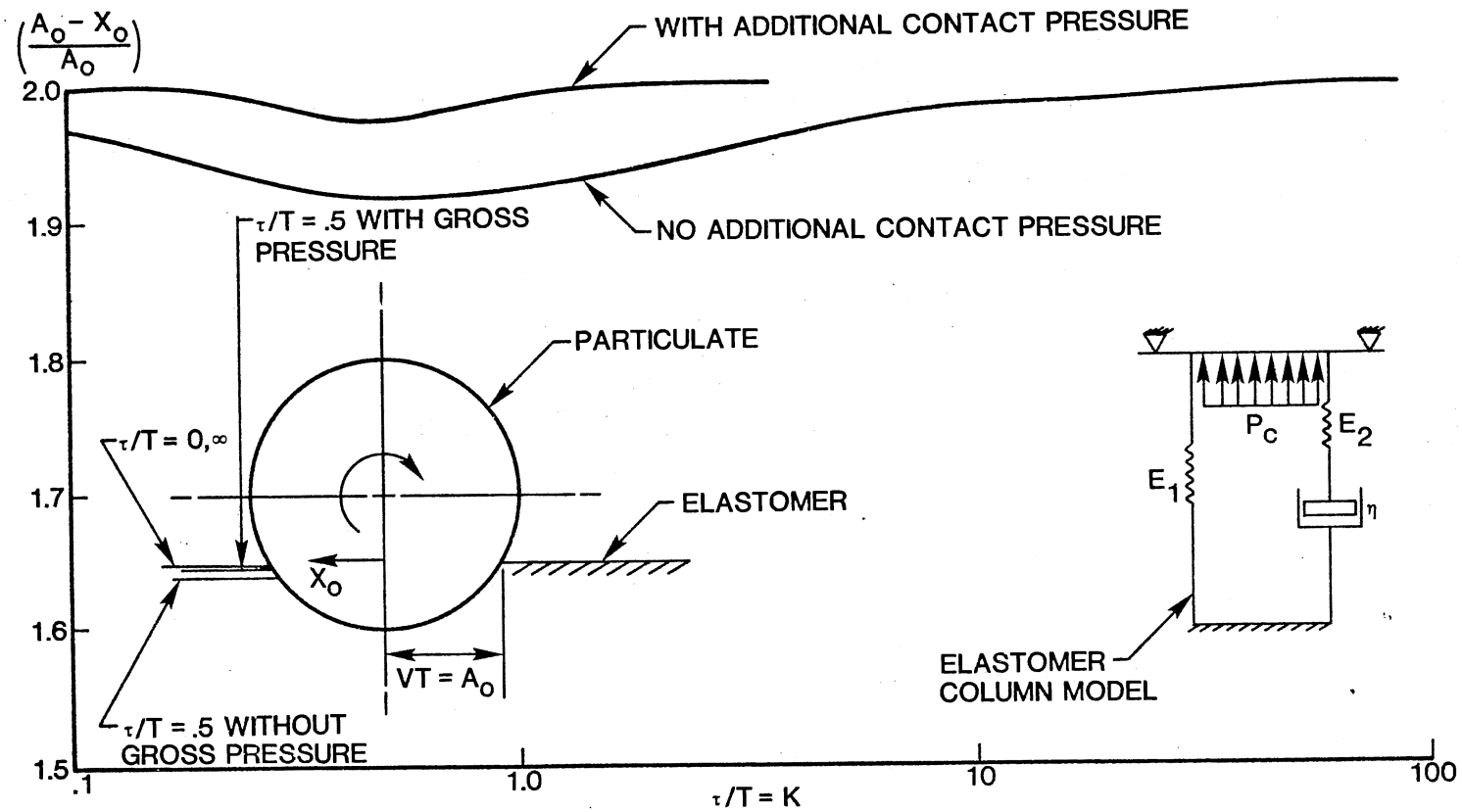
Figure 16. Elastomer Contact Asymmetry as a Function of Relaxation Time and Rolling Velocity.

as a function of time. Substituting the value for t found from Eq. (6-5) into Eq. (6-8) results in

$$F(x) = (E_1/(2r\ell))(2a_0[a_0-x]-(a_0-x)^2)y_0$$
$$dx + (E_2v\tau/(r\ell))[(a_0 + v\tau)(1 - \exp \qquad (6\text{-}19)$$
$$[(x - a_0)/(v\tau)] + x - a_0]y_0dx + P_cy_0dx.$$

where F is now a function of location x and no longer of time t. To sum the moments, F(x) must be multiplied by its moment arm, x, and integrated with respect to x between the limits of x_0 and a_0. Doing so yields

$$M = \int_{x_0}^{a_0} \Big\{ (E_1/(2r\ell))(2a_0[a_0 - x] - (a_0 - x)^2)$$
$$y_0x + (E_2v\tau/(r\ell))[(a_0 + v\tau)(1 - \exp[(x - a_0) \qquad (6\text{-}20)$$
$$/(v\tau)] + x - a_0]y_0x + P_cy_0x \Big\} dx$$

which after an application of integration by parts and a sufficient juggling of the algebra leads to

$$M = (E_1y_0a_0^4/(8r\ell))[1 - 2(x_0/a_0)^2 + (x_0/$$
$$a_0)^4] + (E_2y_0a_0^4/(r\ell))k \Big\{ k^3 - k/2[1 +$$
$$(x_0/a_0)^2] + 1/3[1 - (x_0/a_0)^3] - k(k + 1) \qquad (6\text{-}21)$$
$$(k - x_0/a_0)\exp[- 1/k(1 - x_0/a_0)] \Big\} + Py_0$$
$$((a_0^2 - x_0^2)/2).$$

Putting $E_1 = 3E_2$ as before and using the knowledge that $a^2 = 2rZ_0$ allows the friction to be found as

$$F = M/r \qquad (6\text{-}22)$$

where F = friction force

and so

$$F = \left(E_2 y_0 Z_0{}^2/\ell\right)\left(3/2 - 3(x_0/a_0)^2 + 3/2(x_0\right.$$
$$/a_0)^4 + 4k\left\{k^3 - k/2[1 + (x_0/a_0)^2] + 1/3\right.$$
$$[1 - (x_0/a_0)^3] - k(k + 1)(k - x_0/a_0)\exp$$
$$\left.\left[- 1/k(1 - x_0/a_0)\right] + 1/4[1 - (x_0/a_0)^2]\right) \qquad (6\text{-}23)$$

where the last term $1/4[1 - (x_0/a_0)^2]$ is obtained by

$$P_c y_0(z_0 - x_0{}^2/(2r)) = P_c y_0(z_0 - x_0{}^2/$$
$$(a_0{}^2/z_0)) = P_c y_0 z_0(1 - (x_0/a_0)^2). \qquad (6\text{-}24)$$

Now if Z_0 is again set equal to 1 and if P_c is again set equal to .25 E_2 then

$$P_c y_0 Z_0(1 - (x_0/a_0)^2) = .25 E_2 y_0 Z_0{}^2/\ell$$
$$[1 - (x_0/a_0)^2] \qquad (6\text{-}25)$$

which is seen to be same as the last term in Eq. (6-23).

Figure 17 is a plot of $F[E_2 y_0 Z_0{}^2/\ell]^{-1}$ as a function of k where X_0/a_0 is calculated from Eq. (6-17). It shows what intuition hinted at, that rolling resistance increases with increasing asymmetry and, for a given rolling velocity, the addition of a contact pressure to the viscoelastic system results in increased rolling resistance by the elastomer. The rolling friction drops off to zero, as seen in Figure 17, whenever rolling speed is high enough or low enough to cause the dashpot to become essentially inoperative. It is also observed that for small enough and large enough rolling speeds, the rolling resistance is the same whether contact pressure is present or not. This, as hinted earlier, occurs since at these rolling speeds, the elastomer is being deformed at the same rate

The vertical axis is labelled $F\left[\dfrac{E_2 y_0 Z_0^2}{\ell}\right]^{-1}$ with gridline values .6, .5, .4, .3, .2, .1, 0.

STANDARD LINEAR SOLID WITH
ADDITIONAL CONTACT PRESSURE

STANDARD LINEAR SOLID WITHOUT
ADDITIONAL CONTACT PRESSURE

$K = \tau/T$
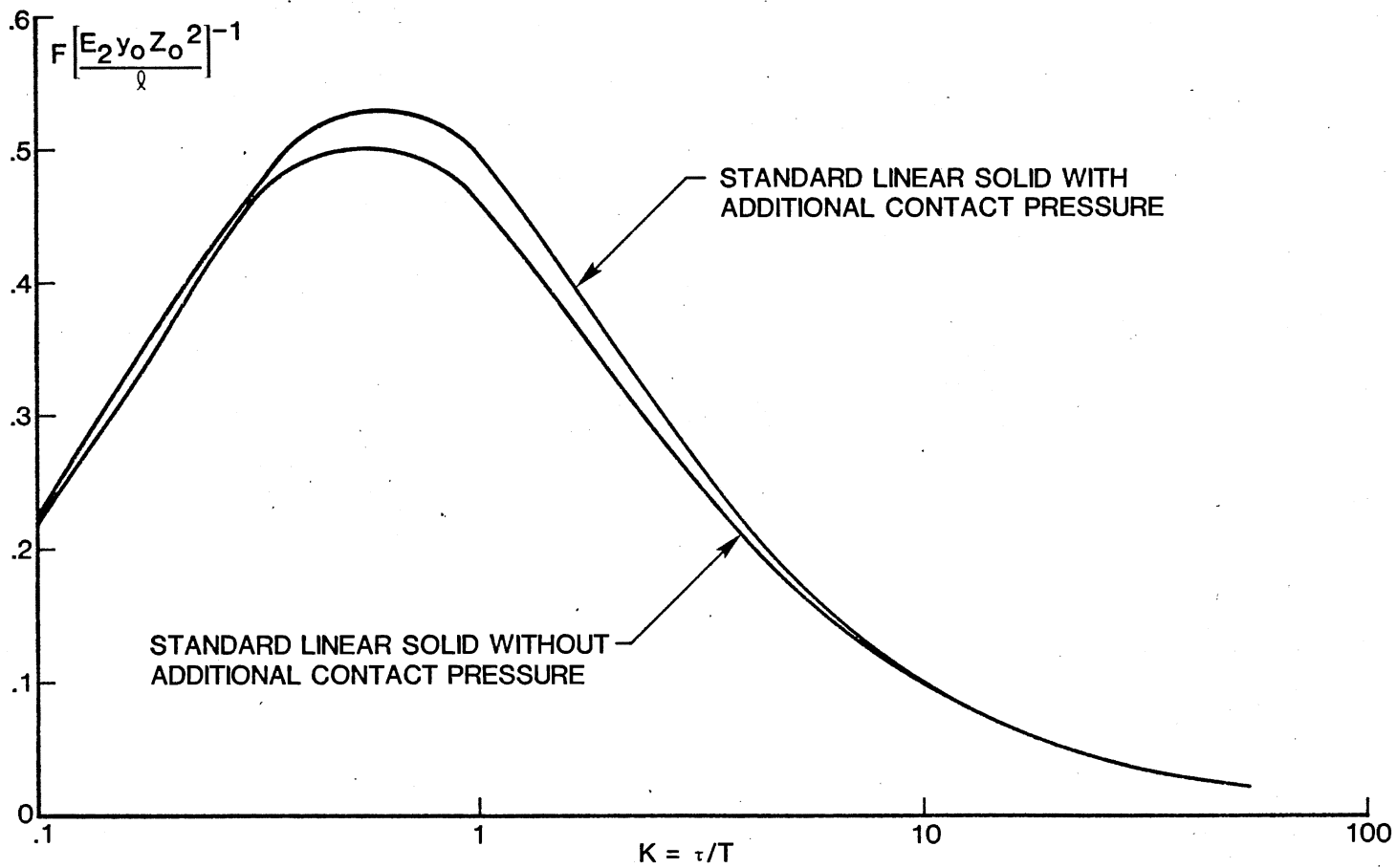
Figure 17. Rolling Friction as a Function of Relaxation Time and Rolling Speed.

regardless of whether or not contact pressure is present and thus the dashpot will then dissipate the same amount of energy.

To evaluate the coefficient of rolling friction, the load on the cylinder as it varies with speed and relaxation time at a constant depth of penetration is derived. Integrating Eq. (6-19) between the limits of x_0 and a_0 with respect to x yields

$$W = \int_{x_0}^{a_0} F(x)dx$$

$$= E_1 y_0/(2r\ell) \int_{x_0}^{a_0} (a_0^2 - x^2)dx + E_2 v\tau y_0/$$

$$(r\ell) \int_{x_0}^{a_0} [(a_0 + v\tau)(1 - exp[(x - a_0)/$$

$$(v\tau)] + x - a_0]dx + \int_{x_0}^{a_0} P_c y_0 dx$$

(6-26)

and

$$W = E_1 y_0 a_0^3/(6r\ell)[2 + (x_0/a_0)^3 - 3(x_0/a_0)]$$

$$+ E_2 v\tau y_0/(r\ell)[(v\tau + a_0)\{a_0 - x_0 + v\tau(exp$$

$$[(x_0 - a_0)/(v\tau)] - 1)\} - (a_0 - x_0)^2/2]$$

$$+ P_c y_0 (a_0 - x_0).$$

(6-27)

Now putting $E_1 = 3E_2$ as before and remembering that $a_0^2 = 2rZ_0$, the load may be expressed as

$$W = (2)^{3/2} E_2 y_0 r^{1/2} Z_0^{3/2} \{1 + 1/2(x_0/a_0)^3$$

$$- 3/2(x_0/a_0) + 2k[1 - (x_0/a_0)^2] + (1/8)$$

$$(1 - x_0/a_0)\}$$

(6-28)

where the last term $(1/8)(1 - x_0/a_0)$ is the contribution due to the contact pressure and letting $P_c = .25 E_2$ and $Z_0 = 1$. This equation is presented graphically in Figure 18.

$$W \left[\frac{E_2 y_o r^{1/2} z_o^{3/2}}{\ell} \right]^{-1}$$

STANDARD LINEAR SOLID VISCOELASTIC
SYSTEM WITH CONTACT PRESSURE

STANDARD LINEAR SOLID VISCOELASTIC
SYSTEM WITHOUT CONTACT PRESSURE

$K = \tau/T$
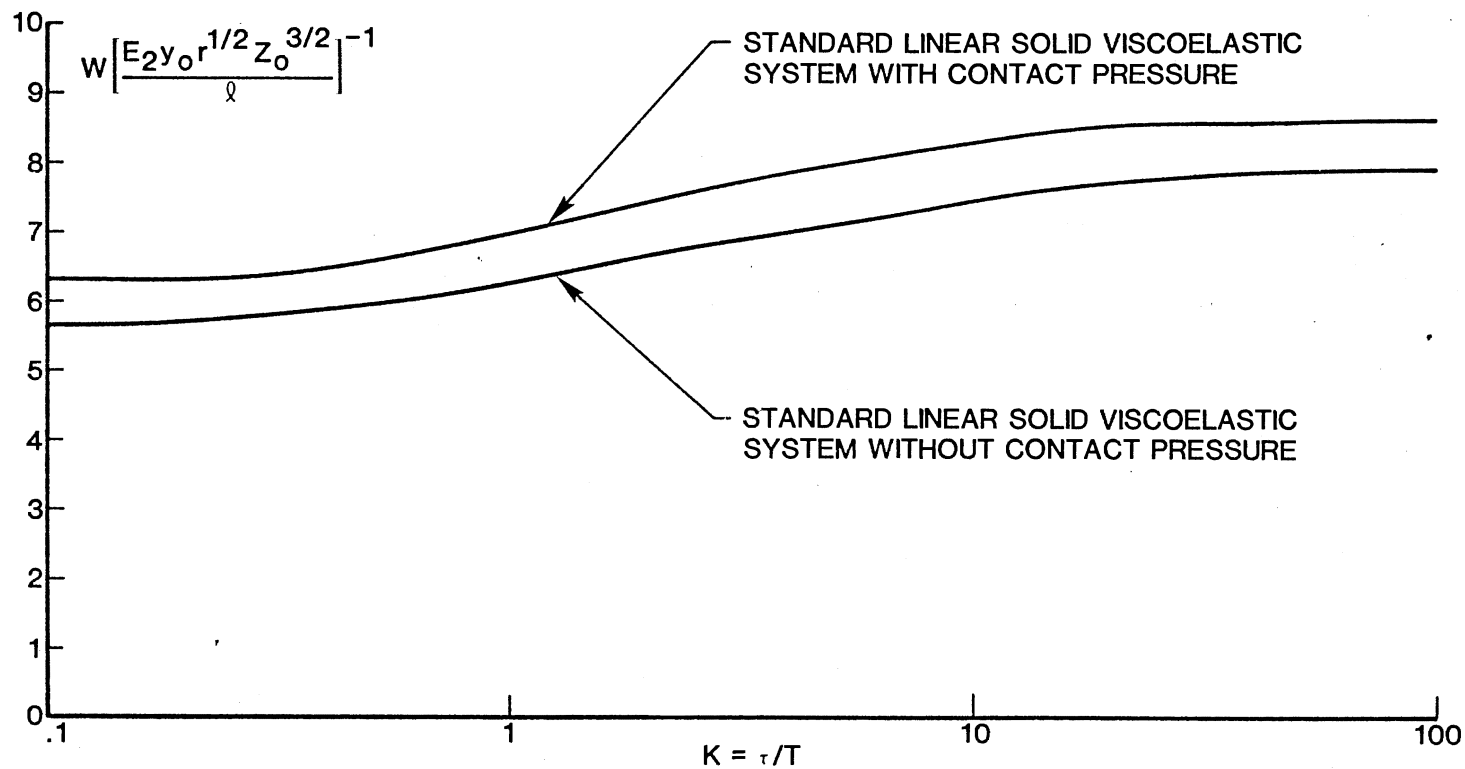
Figure 18. Elastomer Normal Load on a Cylindrical Particle as a Function of
Relaxation Time and Rolling Velocity.

The final point of interest is in knowing what effect contact pressure has on the coefficient of rolling resistance or friction. The coefficient of resistance is given by

$$\mu_r = F/W \qquad (6\text{-}29)$$

where μ_r = coefficient of rolling resistance. The value of $\mu_r (Z_0/r)^{-1/2}$ is presented gaphically against k in Figure 19. It is seen that the addition of a contact pressue P_c to the standard linear solid viscoelastic system reduces the coefficient of rolling resistance. This makes good sense intuitively sinceas contact pressure increases, a more symmetrical draping of the elastomer about the roller occurs which tends to cause all energy losses and hence rolling resistance to reach a specific lower limit at a constant rolling speed. Thus, for a steady energy loss at a constant rolling speed, as load increases due to increasing contact pressure, the coefficient of rolling resistance must decrease.
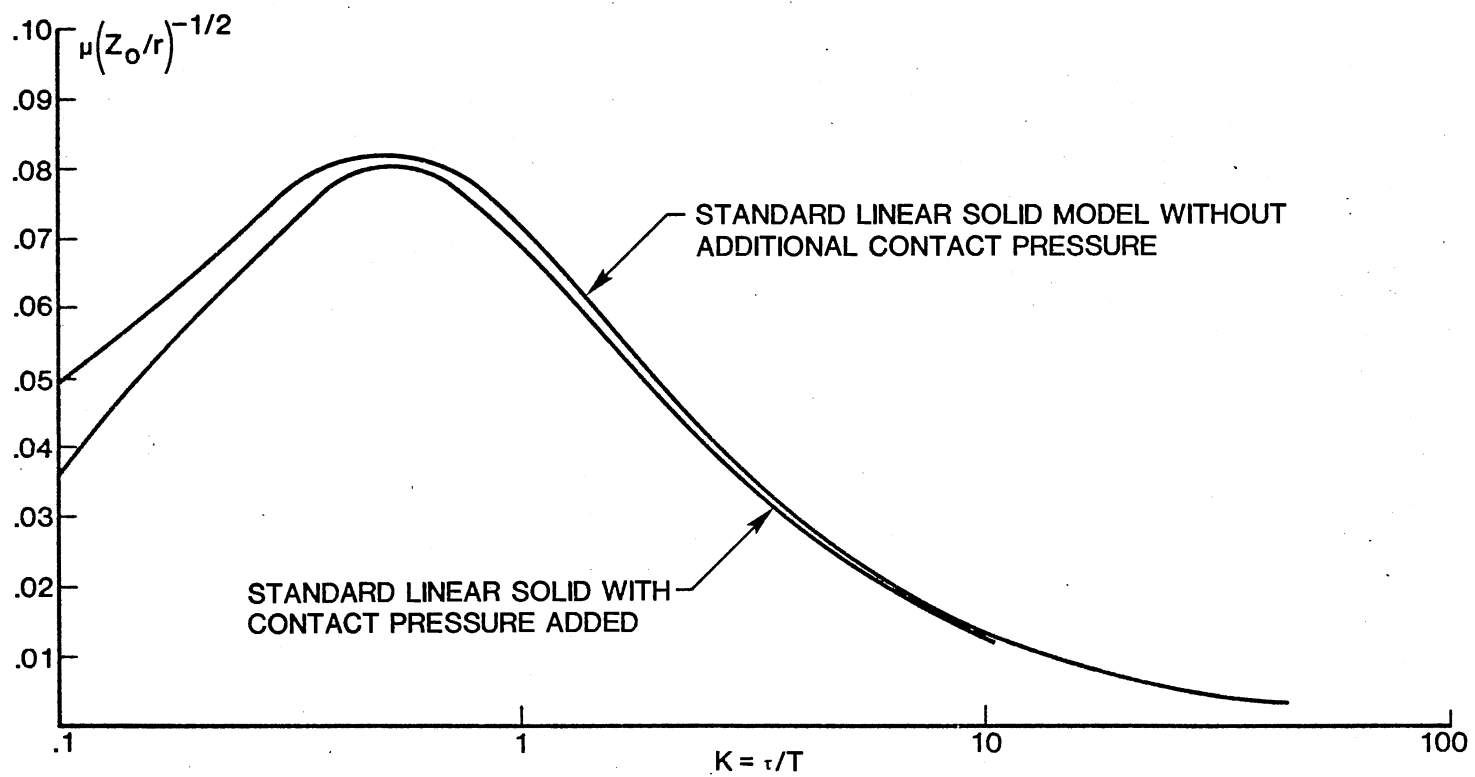
Figure 19. Coefficient of Rolling Friction for a Cylindrical Particulate as a Function of Relaxation Time and Rolling Speed.

CHAPTER VII

PARTICULATE INGRESSION PAST LINEAR SEALS

In trying to discover how many particulates may pass a seal, it is first helpful to assume an ideally elastic elastomer, one which exerts no resistance to the rolling of particulates about on its surface. Assume no slippage between particulate and elastomer or between particulate and rod. For this condition, as shown in Figure 20, the particulate will translate at one-half the speed of the rod.

Since the particulates are assumed small compared with the circumference of the rod, it is appropriate to replace the circumference by a flat sheet of equal width. Figure 21 shows the circumferential sheet with the maximum number of particulates of one size loaded onto it (assume the entire sheet is loaded) prior to its passing beneath the elastomer. The maximum number of particulates which may be spaced one deep about the circumference is

$$C/d = N \tag{7-1}$$

where C = circumference;

    d = particle diameter;

    N = number of particle about the circumference.

As shown in Figure 22, the speed of any particulate while under ideal elastomer influence is one-half that of the rod speed. Figure 22 shows two particulates of equal diameter. One particulate has

FORCE VECTORS
ACTING ON
PARTICULATE

INSTANTANEOUS
CENTER OF ROTATION

IDEALLY
ELASTIC
ELASTOMER

1/2 V

V
ROD VELOCITY
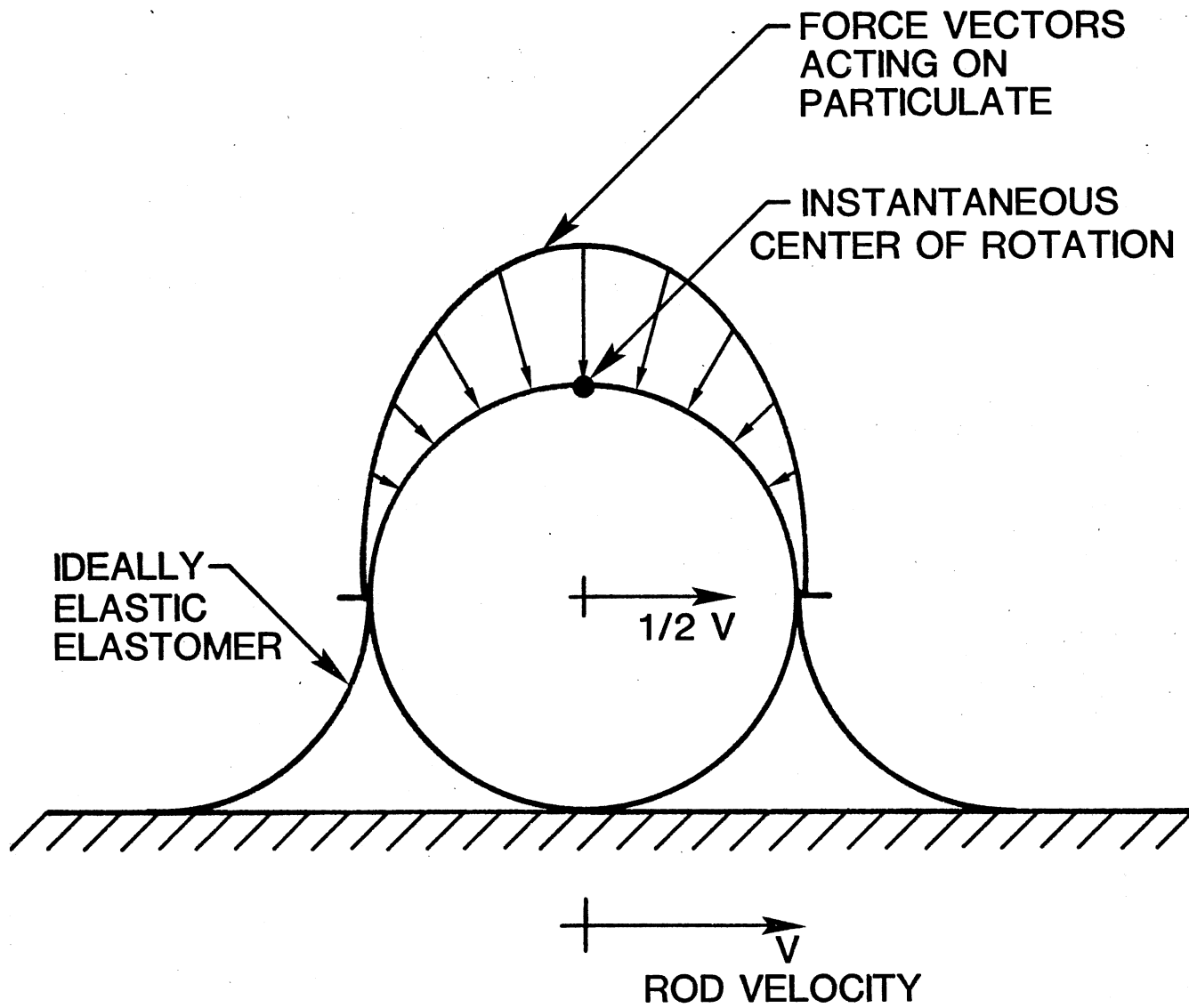
Figure 20.   Ideal Elastomer Force Diagram on a Spherical Particulate.

been in contact with the elastomer over a distance d. This particulate
will take a certain amount of time to traverse the elastomer. When
the other particulate reaches the location originally occupied by the
first particulate, it too will then traverse the elastomer from that
location in the same amount of time taken by the first particulate
from that location. The difference then between the time for the
second particulate to traverse the seal as opposed to the time taken
by the first particulate is then

$$d/(v/2) = T \qquad (7-2)$$

where T is time between when the first and second particulates
traverse the elastomer.

Once the first particulate has traversed the elastomer, it
becomes free of its influence and its speed becomes that of the rod.
Hence, it travels a distance equal to TV before the second particu-
late also becomes free of elastomer influence. The distance
between their centers then becomes

$$TV = [d/(V/2)]V = 2d. \qquad (7-3)$$

Thus, particulates of equal size, upon passing beneath an ideally
elastic elastomer become spaced a distance apart such that an ad-
ditional particulate of the same size could be placed between them.
This shows that, at best, fifty percent of the area of a rod upon
passing a seal will be taken up with particulates. For particu-
lates of different sizes, the value of d may be replaced by the
distance between their centers when the particulates are in contact.
For non-ideally elastic elastomers of the kind discussed in Chapter
VI, the spacing could be even greater since the particulates will
not necessary move at one-half the speed of the rod.

Another point of interest is that there is a certain rod stroke
length necessary before the first particulates coming into contact
with the elastomer, as shown in Figure 22, will traverse the elastomer
and make their presence known on the other side. For an ideally
elastic elastomer, this distance will be

$$v[\ell/(v/2)] = 2\ell = L \tag{7-4}$$

where ℓ = elastomer length;

   L = stroke length prior to detection of any particulates

      passing the seal.

Once this distance, L, is traversed, the particulates will deposit
themselves as discussed above. This distance L will be increased
by some amount for elastomers exhibiting non-ideality as those dis-
cussed in Chapter VI.

Equation (7-3) shows an extremely important part of the answer
to the question of why it is that seals seem to discriminate among
particles as to their willingness to let some sizes pass easily
while other sizes seem to pass much less easily. For the conditions
shown in Figures 20, 21, and 22, Eq. (7-3) shows that, at best, the
spacing between two circumferential rings of particulates is a
minimum of 2d between their centers. That is, if there is room
for M circumferential particulate rings, only .5 M rings will be
present. Now, if there is room for M rings of particulates one
micrometre in size, there is room for only .1 M rings of particulates
10 micrometres in size. If there is room for N one-micrometre
particulates in a circumferential ring, there is room for only .1 N
10-micrometre particulates in a circumferential ring. Thus, while
there may be room for MN one-micrometre particulates,there is
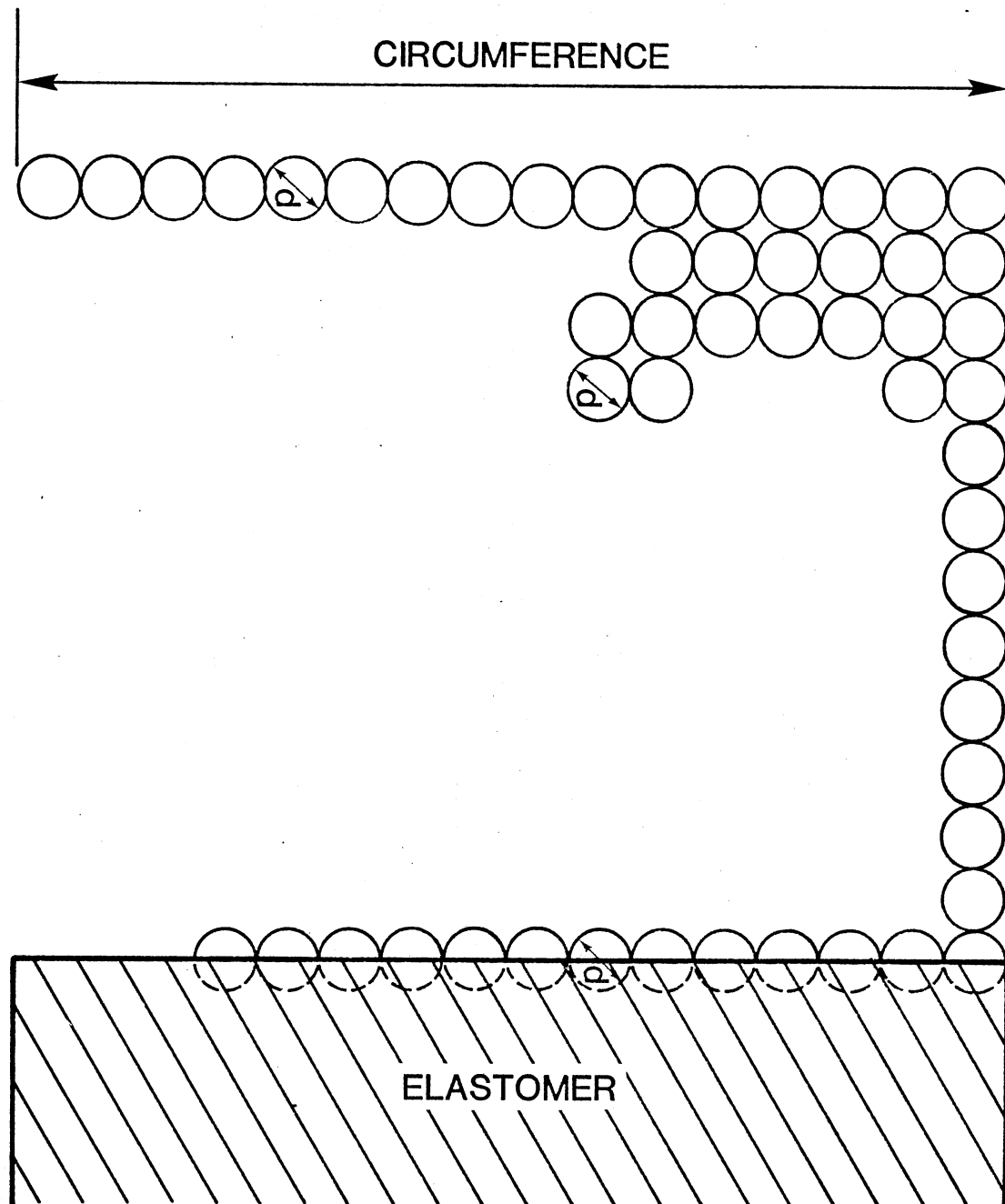
Figure 21. A Circumferential Mono-Sized Particulate Sheet.
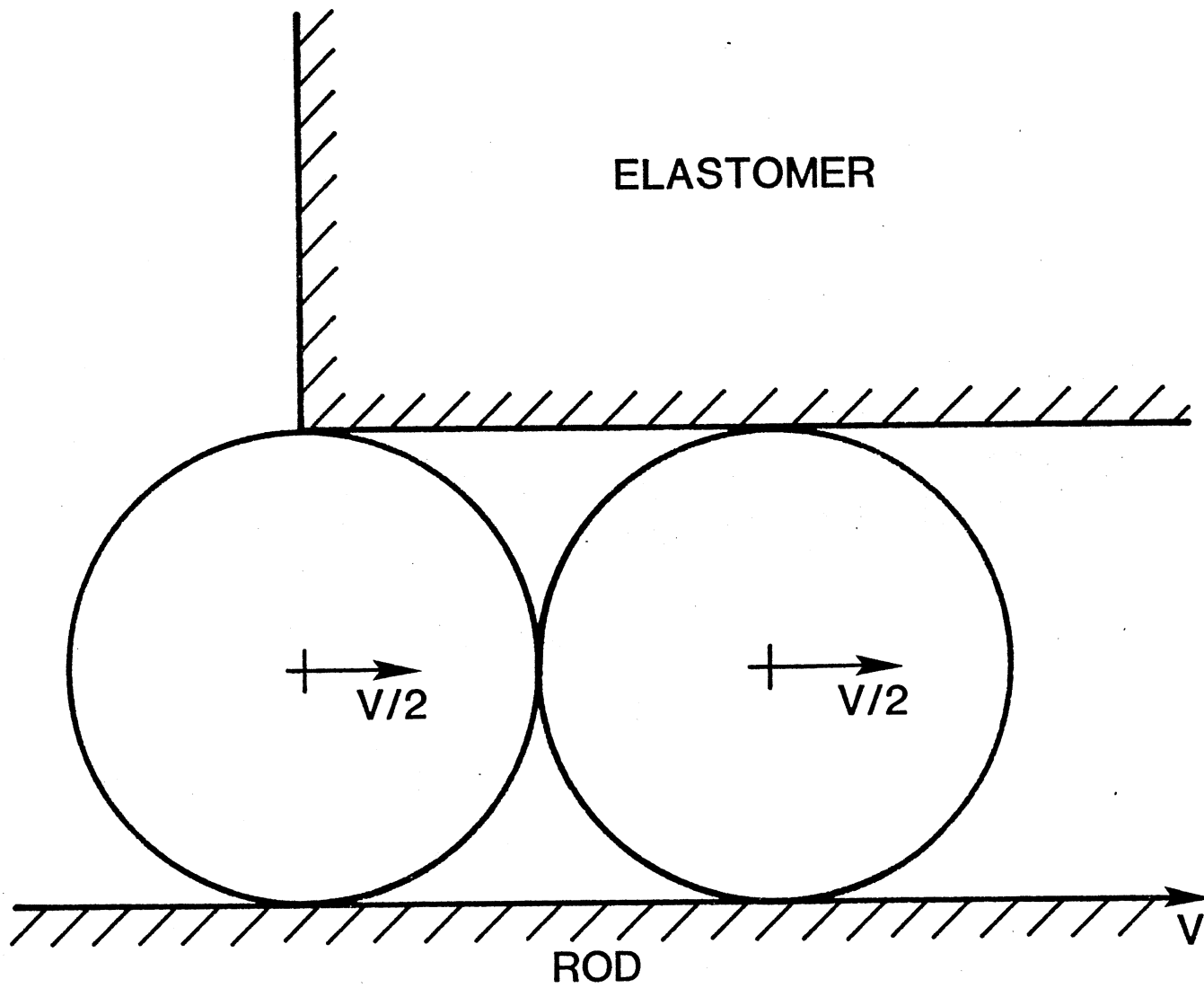
Figure 22. Two Particulates in Intimate Contact Beneath the Elastomer.

room for only (.01) MN 10 micrometre particulates or one percent of the room available for one-micrometre-sized particulates. Thus, for an ideally elastic elastomer, there is the possibility of passing as many as .5(c/1 micrometre)(ℓ_s/1 micrometre) one-micrometre particulates, and for 10-micrometre particulates, there is the possibility of passing only (.005)(c/1 micrometre)(ℓ_s/1 micrometre) where C is the circumference and ℓ_s is the stroke length after passage of the first particulate ring. It is apparent that even ideally elastic elastomers offering no resistance to rolling whatsoever heavily favor the passage of smaller size particulates. So, there is only one percent of the room available for 10-micrometre in size; for 20-micrometre particulates, there is only one-fourth of one percent of the room available as opposed to one-micrometre-sized particulates; and for 50-micrometre-sized particulates, there is only four one-hundredths of one percent of the room available.

The number of particulates of a certain size passing the elastomeric seal is then seen to be proportional to circumference, stroke length (minus a small error term) and inversely proportional to particle size squared.

$$N \alpha C \ell_s / d^2. \tag{7-5}$$

To find out how the form of Eq. (7-5) varies when non-idealities are present, a dimensional analysis will be performed.

The idea of a dimensional analysis is to find certain relations, without using a detailed solution, which must be satisfied by various measurable quantities in which one is interested. A three-part procedure is used in the dimensional analysis: first, a list of all the quantities on which it may be supposed that the answer will de-

pend is made; secondly, all the dimensions of the quantities are written down; thirdly, a demand is made that a functional relation between the quantities be found such that the relation remains true no matter what the size of the units in terms of which the quantities are measured.

Sometimes a dimensional constant is included in a dimensional analysis. A dimensional constant is one which changes in numerical magnitude when the size of the fundamental units changes. Dimensional constants must have dimensional formulas expressible as powers of the primary quantities.

The assignment of numerical magnitudes to measurable quantities involves some system of rules of operation such that the quantities are assigned to one of two groups, which are called primary and secondary. A secondary quantity is defined by a functional relationship of primary quantities. The exponent of the power of any primary quantity is defined as the dimension of the secondary quantity in that primary quantity. The dimensions of a primary quantity are its own corresponding dimensional symbol. The dimensions of a primary quantity have no absolute significance. Thus the primary quantities of two feet and five seconds have the dimension of length and time respectively. The secondary quantity 2/5 feet per second has then dimensions of length to the first power and time to the negative unity power because these are the dimensions of the secondary quantity in the primary quantities. It is, of course, actually meaningless to talk of dividing a length by a time. It is only numbers which are the measure of these quantities.

It is possible for a unit to experience a change different

from that of merely changing the sizes of the primary units. In
going from one system of measurement to another, the primary units
may change in character as well as in size. In each system, all
secondary quantities are expressed in terms of the primary quanti-
ties peculiar to the system and the two systems are consistent. For
example, force is still equal to mass times acceleration in each
system.

A complete equation is a functional relationship between
measureable quantities and dimensional constants which remains
formally true with no change of functional form when the size of
the fundamental units is changed in any way whatever.

An equation may be correct and an adequate expression of
physical facts and yet not be complete. This is contrary to what
is usually stated but what is usually stated is incorrect. How-
ever, every adequate equation may easily be made complete. The
assumption of completeness as a starting point in dimensional analy-
sis is then no hardship. This is very nice because a dimensional
analysis can only deal with complete equations. The size of the
primary units is allowed to change but not the character.

If there exists a complete equation

$$\phi(\alpha, \beta, \gamma, ---) = 0 \qquad (7\text{-}6)$$

its solution has the form

$$F(\pi_1, \pi_2, \pi_3 ---) = 0 \qquad (7\text{-}7)$$

where there are n-m independent π products of the argument α, β, ---,
etc. which are dimensionless in the primary units. Here n is the
number of arguments α, β, γ, ---; m is the number of primary units.
Equation (7-7) is known as the Jeans-Buckingham Pi Theorem. The

solution of Eq. (7-7) may be solved for any one of the π products as shown by

$$\alpha = \beta^{X1}\gamma^{X2} \text{ --- } \phi(\pi_2, \pi_3, \text{ --- })\qquad(7\text{-}8)$$

where the x's are such that $\alpha\beta^{-X1}\gamma^{X2}$---is dimensionless. Equation (7-8) is the mathematical statement of the principle of dimensional homogeneity. The result of a dimensional analysis as formally outlined in Eqs. (7-6) through (7-8) places no restrictions on the form taken by a function which expresses the results of the arguments. The only restriction is on the form of the arguments.

The preceeding discussion of dimensional analysis was based on the book by Bridgman [25]. The application of dimensional analysis chiefly involves use of the Buckingham Pi Theorem. An excellent systematic use of the Buckingham Pi Theorem is outlined by Giles [26]. It states:

> Where the number of physical quantities or variables equals four or more, the Buckingham Pi Theorem provides an excellent tool by which these quantities can be organized into the smallest number of significant, dimensionless groupings from which an equation can be evaluated. The dimensionless groupings are called Pi terms. Written in mathematical form, if there are n physical quantities q (such as velocity, density, viscosity, pressure, and area) and k fundamental dimensions (such as force, length, and time or mass, length and time), then mathematically
>
> $$f_1(q_1, q_2, q_3, \text{---}, q_r) = 0$$
>
> This expression can be replaced by the equation
>
> $$\phi(\pi_1, \pi_2, \pi_3, \text{---}, \pi_{n-k}) = 0$$
>
> where any one π-term depends on not more than (k+1) physical quantities q and each of the π-terms are indepdent, dimensionless monomial functions of the quantities q.
>
> 1. List the n physical quantities q entering

into a particular problem, noting their
dimensions and the number k of fundamental
dimensions. There will be (n-k) π-terms.

2. Select k of these quantities, none dimen-
sionless and no two having the same dimen-
sions. All fundamental dimensions must be
included collectively in the quantities
chosen.

3. The first π-term can be expressed as the
product of the chosen quantities each to
an unknown exponent, and one other quantity
to a known power (usually taken as one).

4. Retain the quantities chosen in (2) as re-
peating variables and choose one of the
remaining variables to establish the
next π-terms. Repeat this procedure for
the successive π-terms.

5. For each π-term, solve for the unknown
exponents by dimensional analysis.

Helpful Relationships:

a. If a quantity is dimensionless it is a
π-term without going through the above
procedure.

b. If any two physical quantities have the
same dimensions, their ratio will be one of
the π-terms. For example, L/L is dimension-
less and a π-term.

c. Any π-term may be replaced by any power
of that term, including π^{-1}. For example,
π_3 may be replaced by $\pi_3{}^2$, or π_2, by $1/\pi_2$.

d. Any π-term may be replaced by multiplying
it by a numerical constant. For example,
π_1 may be replaced by $3\pi_1$.

e. Any π-term may be expressed as a function
of the other π-terms. For example, if there
are two π-terms, $\pi_1 = \phi(\pi_2)$. (pp. 57-58)

With this procedure as a guide, a dimensional analysis will be

made to determine the forms of various relations between particulate

size, rod velocity, stroke length, surface tension, and seal length,

squeeze, and viscoelastic properties.

When conducting a dimensional analysis, one must decide on which physical variables are important determining factors in the problem. For example, in the determination of the number of particles of a certain size which will pass an elastomeric seal during relative motion between the seal and its mating surface, that is, the cylinder rod, one would hardly include gravity as one of the physical quantities upon which the answer lies. A list of physical variables appropriate to the problem is as follows:

TABLE I

Physical Quantity	Symbol	Dimensions
Percent Squeeze	S	---
Coefficient of Rod Particulate Friction	μ	---
Number of Particles of Size d	N	---
Stroke Length	ℓ	L
Rod Circumference	C	L
Particle Size	d	L
Rod Velocity	V	LT^{-1}
Relaxation Time	τ	T
Contact Pressure	P_c	FL^{-2}
Young's Modulus	E	FL^{-2}
Surface Tension	σ	FL^{-1}
Totals	11 quantities -	3 fundamental dimensions = 8 π-terms

By inspection, S, μ, N, ℓ/d, C/d, $V\tau/d$, P_c/E and $\sigma/(Ed)$ are the

eight dimensionless π-terms. Solving for one π-term, N, in terms of all the other π-terms yields

$$N = f(S, \mu, \ell/d, c/d, v\tau/d, P_c/E, \sigma/(Ed)). \qquad (7\text{-}9)$$

Now it can be argued that for all conditions that doubling the stroke length or doubling the rod circumference will double the number of particulates passing the seal. With this additional assumption, Eq. (7-9) becomes

$$N = \ell c/d \; f(S, \mu, v\tau/d, P_c/E, \sigma/(Ed)). \qquad (7\text{-}10)$$

Equation (7-10) indicates that doubling the rod velocity has the same effect on N as doubling the relaxation time. Similarly, doubling P_c has the same effect as halving E and σ.

Some of the physical quantities in the preceding list may actually be unimportant in determining the number of particulates of a certain size, N, which will pass the seal. For example, the surface tension, σ, is more concern in answering the question of the possibility of particulate passage and not quantity of that passage, so the suface tension, σ, should be dropped.

Percentage squeeze, S, is related to the question of whether a particulate may even start its journey past the seal due to its influence on the entrance zone. Since it is related also to the value of the contact pressure, P_c, S may be dropped from the analysis. Now the relaxation time, τ, is really a measure of elastomer elastic imperfection, that is, the viscosity present in an elastomer. Let τ be replaced by the elastomer viscosity, η. Young's modulus, E, may be dropped from the list as the contact pressure, P_c, is either determined by it to a large extent or overrides E such that E is of

minor importance. So, the modified list becomes:

TABLE II

Physical Quantity	Symbol	Dimensions
Coefficient of Rod Particulate Friction	μ	---
Number of Particles of Size d	N	---
Stroke Length	ℓ	L
Rod Circumference	C	L
Particle Size	d	L
Rod Velocity	V	LT^{-1}
Elastomer Velocity	η	FTL^{-2}
Contact Pressure	P_c	FL^{-2}
8	-	3 = 5 π-terms

By inspection, μ, N, ℓ/d, C/d, and $(dP_c)/(V\eta)$ are the five dimensionless π-terms. Solving for N in terms of the other π-terms yields

$$N = f(\mu, \ell/d, \; c/d, \; (dPc)/(V\eta)) \qquad (7\text{-}11)$$

And because of reasons assumed previously, Eq. (7-6) may be written as

$$N = \ell c/d^2 f(\mu, \; dP_c/(V\eta)) \qquad (7\text{-}12)$$

Equation (7-12) indicates that doubling the rod velocity has the same effect as halving the contact pressure. Using the results of Chapter VI, the second π-term, $\pi_2 = (dP_c)/(V\eta)$ can be represented

differently. Allowing n/P_c to be sort of relaxation time, π_2 can be represented by

$$\pi_2 = dP_c/(Vn) = d/[(a_0/T)\tau_c] = (d/a_0)/K_c \qquad (7\text{-}13)$$

where a_0 = the semi-length of contact as shown in Figure 14;

$\quad$ T = the time taken by the particulate in moving a distance a_0;

$\quad$ K_c = the ratio k based on contact pressure.

Since a_0 is related to d, Eq. (7-13) becomes

$$\pi_2 = C_1/K_c = K_c \qquad (7\text{-}14)$$

where the use of helpful relationships c and d were used and C_1 is a constant. Now N is seen to be a function of rod-particulate friction coefficient and a term K_c.

$$N = \ell c/d^2 f(\mu, K_c) \qquad (7\text{-}15)$$

Equation (7-10) is very valuable. It can now be shown by again doing a dimensional analysis using ℓ, C, d, and K_c/μ as the physical quantities and again assuming the relationships between ℓ, C, and d as before that

$$N = \ell c/d^2 f(\mu/K_c). \qquad (7\text{-}16)$$

Equation (7-11) shows that increasing the rod-particulate coefficient of friction by some factor results in the same effect on the number of particulates passing the seal as does reducing K_c by the same factor.

It was seen in Chapter VI that the coefficient of rolling resistance was a function of both K and P_c; and, hence, it is a function of K_c. Now the coefficient of rolling resistance in Chapter VI was based on a force acting at the centroid. The peripheral speed of the particulate will match the speed of the rod then whenever

$$\mu \geq f_{rr}(K_c)/2 \qquad\qquad (7\text{-}17)$$

where f_{rr} = coefficient of rolling resistance as function of K_c.

When this occurs, particulates will translate at one-half the rod velocity. N then becomes a function of ℓ, C, and d only, with ℓ being in error by a length roughly the length of seal contact with the rod.

Equations (7-11) through (7-17) and their associated reasoning applies to those particles of a size able to first transit the entrance zone. Of additional interest in Eq. (7-12), elastomer viscosity, η, becomes inconsequential as P_c increases as shown in ChapterVI. As rod velocity V decreases, η may become larger or P_c smaller without affecting N as shown in Chapter VI. The effect of changing d is not discernable for a non-ideal elastomer since d is both outside and under the function sign in Eq. (7-12).

CHAPTER VIII

LEAKAGE VERSUS INGRESSION

The list at the end of Chapter II delineated the findings and/or beliefs of several investigators as to what influences the transport of particulates past an elastomer which is pressed with an interference fit on to an inelastic solid surface. One finding of very great interest to the manufacturers and users of reciprocating linear motion hydraulic pressure seals was that a seal which leaks more allows less ingression of particulates than a seal which leaks less. This unexplained phenomenon can now be readily explained.

Leakage has been known to be caused by differences in the thicknesses of the fluid films passing a pressure seal between the directions of stroke since the 1940's. A non-leaking seal may therefore, exude a very thick film of fluid on one stroke and, if it all passes again beneath the seal on the return stroke, the seal is defined as non-leaking. The pressures beneath the seal, when no relative motion is occuring, and the entrance zone combine to produce a film pressure having inflection points on both sides during relative motion between the seal and its mating surface. It is the gradient in the film pressure profile at the inflection point facing toward the moving mating surface which determines how much fluid will pass the seal. The smaller the gradients, the more fluid will pass and, hence, the thicker will be the film of fluid.

Generally, pressure seals operate under conditions where for one stroking direction, the film pressure profile closely approximates the stresses in the elastomer due to its interference fit with the rod, while that for the opposite stroke is distorted due to a high pressure on one side of the seal. This usually results in leakage because the gradient at the inflection point is a smaller value as the rod extends outward causing a thick oil film, while it is a larger value as the rod returns past the seal causing a thinner oil film. A seal which leaks less may do so by either emitting a thinner oil film, allowing back a thicker oil film, or doing both in combination. To put out an initially thinner film may allow capillarity forces to assume a bigger role and this could be one reason why seals which leak less were discovered to ingress more particulates.

A seal which allows back a thicker film of fluid does so generally by decreasing the gradient of the film pressure profile at the inflection point by use of a tapering entrance zone. The longer the taper and the smaller the angle, the higher it is known that the pressure becomes from elementary lubrication theory. Because the stress in the elastomer surface is a monotonic decreasing function when no relative motion is taking place, by boosting the pressure in the entrance zone higher and higher, it blends in to the original stress profile at a point of ever decreasing gradient. This results in a thickening of the fluid film and a resulting decrease in the leakage. This same slow taper which promotes less leakage also allows large particles to enter the seals interfacial zone as discussed in Chapter III. Thus, it is very reasonable for seals which leak less to ingress more contaminants than seals which leak more.

Another similar point in Chapter II was that the hardest thing to seal against particulate ingression was a mud slurry. Part of the

reason for this was shown in the preceding chapter. When particulates are closely spaced on one side of a seal of ideal elastic properties, they will cover 50 percent of the surface area of the rod on passing through the seal if they can first pass the entrance zone. If the particulates are not compactly placed around the circumference, less will pass than can pass for a compactly placed mud slurry.

CHAPTER IX

EXPERIMENTAL ANALYSIS

Several findings and theoretical suppositions were outlined in
Chapter II in regard to particulate ingression past elastomeric
linear seals. The next several chapters were an attempt to theo-
retically determine to what extent those findings and suppositions
were justified. Each of the ten summary findings and theoreti-
cal suppositions outlined at the end of Chapter II were considered
in the text. It is the purpose of this chapter to offer experimental
support of the findings of this analysis.

Of special and first importance is the effect of the entrance
zone geometry on a linear elastomeric seal's ability to restrict
particulates. Chapters III, IV, V and VIII were the analysis of
this phenomenon. Forty percent of the chapters of this thesis
were devoted to this topic. This is a correct indication of its
importance when it is considered that if particulates don't pass
through this zone, they cannot get past the seal.

To give support to the developed theory, a test apparatus was
designed and built and tests were conducted. It is a simple machine
whose purpose is to drive a rod through an elastomeric seal housed
in a seal housing. Both the speed and the stroke length may be
varied. Elastomeric seals having different material properties may
be placed in the seal housing.

The test procedure consisted of cleaning the rod, seal housing and seal with filtered petroleum ether. The rod was coated with a thin film of oil by oiling it on one side of an o-ring and moving the o-ring down the length of the rod. The seal housing, seal and rod were all assembled into the test machine. Solid glass spheres approximately 1 to 50 micrometers in size were poured into the annulus between the rod and the bore. For the test conducted to determine the effect of the entrance zone on particulate ingression, the seal was just covered with the glass spheres. For tests conducted to determine the effect of elastomer relaxation time on particulate ingression, the entire annulus was filled with glass spheres to a depth of about one inch. The rod was then driven down through the seal and washed with oil from a wash bottle into a funnel which was placed in a sample bottle. The oil in the sample bottle was then analyzed on an automatic electronic particle counter. The volume of oil in the sample bottle was recorded.

The stroke length for each test was measured and the time of stroke noted. Each sample bottle and the funnel and the wash bottle were checked for cleanliness prior to each test. The funnel was placed in the sample bottle and the oil was added from the wash bottle to fill the sample bottle half full. This sample was then counted by the particle counter.

It was essential in experimental work of this type to perform the experiments under clean conditions. Particulates of the size of interest used in the experiments can easily be found floating about in normal room air and thus the apparatus was located and testing was conducted in the clean room at the Fluid Power Research

Center laboratory. The air in this room is continously exchanged and filtered and affords an excellent place for conducting experiments of this nature. The sample bottles and the wash bottle used in the experiments had to be meticulously clean so as not to bias the experimental results. A standard cleaning procedure developed at the Fluid Power Research Center to clean sampling bottles was used. This consist of ultrasonically cleaning these containers in a vibratory bath filled with hot water and detergent followed by water only rinses in the vibratory bath. Use is made of glacial acidic acid to keep any detergent from adhering to the insides of the containers with a final water rinse using a jet spray of demineralized water. This is followed by an alcohol rinse to remove all traces of any adhering water droplets which is then followed by a final rinse with petroleum ether, applied through a 0.45 microetre pore size filter.

The Particulates used in the experiments were solid glass spheres, the smallest size being approximately 50 micrometres in diameter. The particulates were very spherical in shape when viewed under a microscope and their use eliminated the experimental uncertainty due to varying shaped particulates.

The elastomeric seals used all had circular cross sections of approximately 3/16 of an inch in diameter. It had been the author's intention to use seals of square cross section and machine various entrance zone angles on the seals. Several companies advertising seals of square cross section were contacted but none sold this shape except in very large quantities. The o-ring was then decided upon because it was available in a variety of materials.

The rod used was of standard design being chrome plated with a surface finish of 16 microinches Ra.

The seal housing had a smaller bore at the bottom through which the rod passed and acted as a shelf for the o-ring to sit on. A larger bore at the top was machined to produce a small interference fit on the seal between the rod and the wall of the bore. Varying degrees of interference were produced by placing pieces of shim stock in between the seal and the bore.

Along with the effect of entrance angle on particulate ingression it was thought desirable to judge the validity of Eq. (7-12).

$$N = \ell c/d^2 f(\mu, dP_c/(Vn)) \tag{7-12}$$

where N = the number of particulates of size d;

ℓ = the stroke length;

C = the rod circumference;

d = particualte spherical diameter;

μ = rod-particulate coefficient of friction;

P_c = average contact pressure beneath the elastomer;

V = rod velocity;

n = elastomer viscosity.

The coefficient of rod-particulate friction should have remained relatively constant during the course of the experiments. The same rod was used for all tests, the same types of particulate and the same lubricant. Assuming a constant μ, Eq. (7-12) becomes

$$N = \ell c/d^2 f(dP_c/(Vn)) \tag{9-1}$$

From the analysis of the previous chapters, the value of the function of the non-dimensional grouping of Eq. (9-1) should be predictable

as a limit value as certain of its constituents approach large or small values. The following is a listing of what could be expected based on the analysis of the precious chapters.

$$V \to \infty, \; f \to 1/v, \; N \to 0$$
$$V \to 0, \; f \to 1, \; N \to \ell c/d^2$$

$$\eta \to \infty, \; f \to 1, \; N \to \ell c/d^2$$
$$\eta \to 0, \; f \to 1, \; N \to \ell c/d^2$$

$$P_c \to \infty, \; f \to 1, \; N \to \ell c/d^2$$
$$P_c \to 0, \; f \to ?, \; N \to ?$$

$$d \to \infty, \; f \to d, \; N \to 0$$
$$d \to 0, \; f \to 1, \; N \to \infty$$

The form of graphical plot expected when plotting $f(dP_c/v\eta)$ versus τ_c while holding the other variables constant is shown in Figure 23. In place of P_c and η, the relaxation time

$$\tau_c = \eta/P_c \qquad\qquad (9\text{-}2)$$

will be used where

$$\tau_c \to \infty, \; f \to 1, \; N \to \ell c/d^2$$
$$\tau_c \to 0, \; f \to 1, \; N \to \ell c/d^2.$$

It is important to know what uncertainties can be expected in the measured values of N, ℓ, C, d, τ_c, V, and S, the squeeze. The uncertainty in the length measurement is taken to be equal to one-half of the least count readable on the measuring scale [27, 28]. The tape used had markings one-sixteenth of an inch apart. The uncertainty in any length measurement is then ± 1/32nd of an inch. Stroke length measurements require two measurements from a datum which was taken to be the base of the test apparatus. An initial

$C_2 = d/v$

$f(C_2/\tau_c) = N/\ell c/d^2$
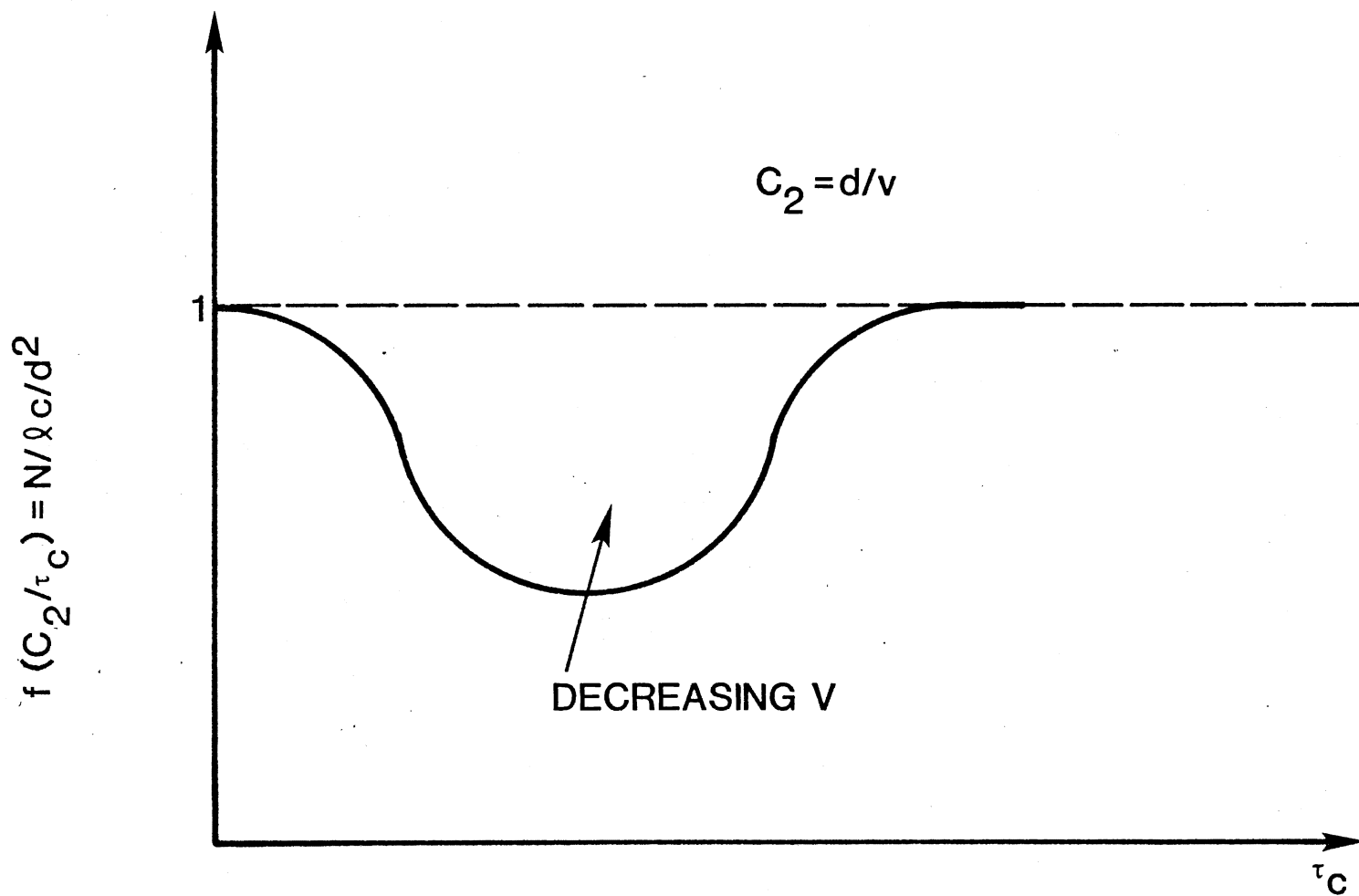
DECREASING V

τ_c

Figure 23. The Theoretical Effect of Elastomer Relaxation Time on Particulate Ingression.

reading is made of the height at the bottom of the rod above the base and another measurement is made after running the run down through the seal. The maximum uncertainty then in the recording of a stroke length is the sum of the uncertainties in each measurement or ± 1/16th of an inch.

The rod circumference was calculated using the formula

$$C = \pi D \tag{9-3}$$

where D = the diameter.

The diameter, D, was measured with a vernier caliper. The caliper can be read to the nearest one-thousandth of an inch which is the least count between markings on the instrument. The uncertainty in the measurement of diameter is then ± .0005 inches. The uncertainty in circumference is then ± .0005 inches.

The value of τ_c is computed by dividing a number which is used as a measure of elastomer viscosity by a number which is used to measure elastomer compression pressure. The compression pressure, P_c, used in the experimental work will be a calculated value based on the following formula

$$P_c = SE \tag{9-4}$$

where S = percent by which the elastomer is compressed;

E = Young's modulus of elasticity.

The percent squeeze, S, is calculated by subtracting from the diameter of the elastomer cross section one-half the difference between the bore diameter and the rod diameter and dividing this value by the original diameter of the cross section. Thus

$$S = \frac{[d_s - 1/2(d_b - d_r)]}{d_s} = 1 - \frac{1}{2}\frac{(d_b - d_r)}{d_s} \tag{9-5}$$

where d_s = the original seal cross-sectional diameter;

d_b = the bore diameter;

d_r = the rod diameter.

Both d_b and d_r are measured with the same caliper and so both d_b and d_r have uncertainties in their measure of ± .0005 inches. The uncertainty in the cross-sectional diameter, d_s, and the cross-sectional diameter of the seals used is given in the maufacturer's catalog as 0.210±.005 inches [29]. The uncertainty in the value of squeeze, S, will then be one-half the value of $S_{max} - S_{min}$.

Young's modulus for the elastomers used in the experiments is found from a graph of International Rubber Hardness Degrees (IRHD) versus Young's modulus. The hardness of the elastomers used in the experiments are designated by the manufacurer in terms of durometer on the Shore A scale. The scales of IRHD and Shore A durometer are comparable [30]. The manufacturer places an uncertainty on the durometer of ±5 points. Thus, the uncertainty range in the value of Young's modulus for the various elastomers with the help of Figure 24 is given with the lower, correct, and upper values.

70 durometer: 830, 1040, 1340 lbf/in^2

75 durometer: 1040, 1304, 1800

90 durometer: 2500, 4000, 6000

95 durometer: 4000, 6000, ----

The viscosity, η, of the elastomers was measured using a Rex Durometer Handheld, Model No. 1700, Serial No. A-12892, durometer measuring device. The gage is used by pressing it firmly onto the elastomer and holding it steadily for 15 seconds. The initial and final readings are read in units of Shore A durometer. The viscos-

ity is found by

$$E_1 + E_2 e^{-t/\tau} = E(t) \qquad (9\text{-}6)$$

where $E_1 + E_2$ = the initial Young's modulus read upon the initial

application of the gage ;

τ = relaxation time of the elastomer modeled as a Voight-

Kelvin model;

t = time in seconds from initial placement of the gage;

and each $E(t)$ is the average of four trials.

$E(0) = E_1 + E_2$

$E(5) = E_1 + E_2 \exp[-5/\tau]$

$E(15) = E_1 + E_2 \exp[-15/\tau]$

Then

$$\frac{E(o) - E(5)}{E(o) - E(15)} = \frac{1 - \exp[-5/\tau]}{1 - \exp[-15/\tau]} \qquad (9\text{-}7)$$

and τ is solved for numerically. The uncertainty arises in the values

for $E(t)$ and in the time, t. The least count on the Rex Shore A

durometer gage is 1 unit and it can be practically read to one unit.

So the uncertainty in a Rex durometer reading is $\pm.50$ units. This is

about±50 psi in the Young's modulus. This should perhaps be com-

bined with a ±250 psi error in reading the value of Young's modulus

from the graph in Figure 24. An error of ±250 psi for each value of

$E(t)$ is perhaps a reasonable estimate. The uncertainty in the time,

t, is one-half the least count on the second hand on a watch which

is $\pm.5$ seconds. The uncertainty in τ is found from

$$\frac{[E(o) - E(5)]\pm 500 \text{ psi}}{[E(o) - E(15)]\pm 500 \text{ psi}} = \frac{1 - \exp[-5/\tau]\exp[\pm.5/\tau]}{1 - \exp[-15/\tau)]\exp[\pm.5/\tau]} \qquad (9\text{-}8)$$

Once a value for τ is found, the viscosity, η, may be found from
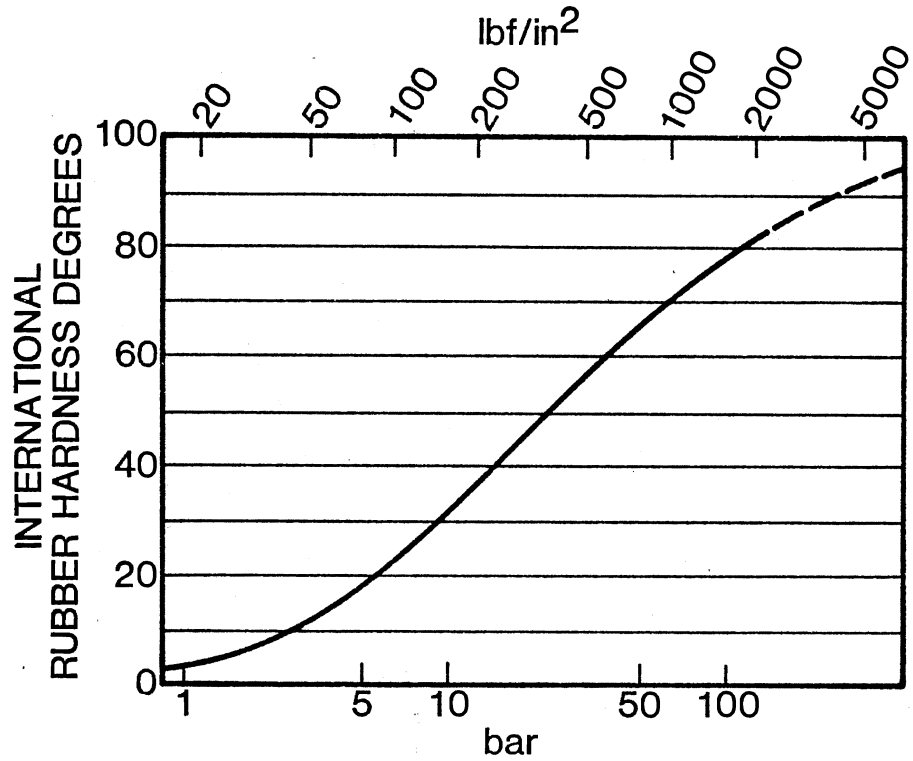
YOUNG'S MODULUS		INTERNATIONAL RUBBER HARDNESS DEGREES
N/mm^2	lbf/in^2	
1.47	213	40
1.76	256	45
2.14	310	50
3.16	460	55
4.34	630	60
5.72	830	65
7.16	1040	70
9.24	1340	75

Figure 24.   The Relationship Between IRHD and Young's Modulus.

$$\eta = \tau(E(o) - E(15)). \tag{9-9}$$

The uncertainty in η is found from

$$\eta_{max} = (\tau + \Delta\tau)(E(o) - E(15) + 500) \tag{9-10}$$

$$\eta_{min} = (\tau - \Delta\tau)(E(o) - E(15) - 500) \tag{9-11}$$

$$\Delta\eta = 1/2(\eta_{max} - \eta_{min}). \tag{9-12}$$

The value of τ_c is calculated from

$$\tau_c = \eta/P_c = \eta/(ES) \tag{9-13}$$

where τ_c = relaxation time based on contact pressure;

P_c = contact pressure based on nominal squeeze;

E = the value of Young's modulus corresponding to the manu-

facturers value for Shore A durometer;

S = squeeze;

The uncertainty in τ_c is given by

$$\frac{1}{2}\left[\frac{(\eta + \Delta\eta)}{(E - \Delta E)(S - \Delta S)} - \frac{(\eta - \Delta\eta)}{(E + \Delta E)(S + \Delta S)}\right] = \Delta\tau_c. \tag{9-14}$$

The velocity, V, has an uncertainty of

$$\frac{1}{2}\left[\frac{(\ell + 0.0625 \text{ inches})}{T - .1 \text{ seconds}} - \frac{(\ell - 0.0625 \text{ inches})}{T + .1 \text{ seconds}}\right] = \Delta V \tag{9-15}$$

where T was measured with a stop watch with a least count of .20 seconds.

The number of particulates, N, is subject to systematic error arising from the fact that after the rod is washed rather equally all over with the wash bottle, it could still contain some particulates. Also, the bottle used to collect the wash fluid and the funnel placed in the bottle to collect the wash fluid contain some particles. The percentage error in the counts was alway under 10

percent and frequently under 5 percent.

The number of particulates counted in a certain size range will be taken to be the number of particulates of a size equal to the mid-size of the range. All counts are made after about 15 minutes of violently shaking the sample bottle in a paint shaker, placing it it an ultrasonic bath for 30 seconds and then subjecting it to vacuum deaeration. This is to disperse the particulates as uniformly as possible and to get rid of any micrometre size air bubbles which would bias the count.

Three counts, one after the other, are made on a HIAC Criterion Automatic Particle Size Analyzer, model PC-320, by Pacific Scientific Company. The particle counter is calibrated according to a method pioneered and developed at the Fluid Power Research Center. The method has been adopted as a standard by the American National Standards Institute (ANSI/B93.28), the National Fluid Power Association (NFPA/T2.96), and the International Standards Organization (ISO/TC131/SC). This standard method is the only approved method of calibration of automatic particles counters by any standards association. The shape of the particle is somewhat a cross between an ellipse and a rectangle (ACFTD, Air Cleaner Fine Test Dust sold by General Motors). Counts can be expected to deviate from the actual number of particles passing through the counter sensor by less than 2 percent [31]. Spherical particles were found to have a correlation with ACFTD of

$$d_S/d_{ACFTD} = 0.65 \qquad\qquad (9\text{-}16)$$

by Pacific Scientific Co. [31].

The average of three counts in succession based on samples of

10 millilitres will be assumed to be the actual count. The uncertainty in this count will be based on sample bottle cleanliness as explained above.

To test the effect of a changing entrance geometry on particulate ingression, a seal was squeezed with an ever-increasing interference. The number of particules in each size range passing the seal per inch of stroke length were determined.

The seal used was made of Nitrile and had a durometer of 90 Shore A as designated by the manufacturer. The bore in the seal housing was measured and it had a value of 2.405 inches. The rod had a circumference of 2.000 inches. The bore diameter was decreased with the introduction of shim stock of 0.001, 0.002, 0.003, 0.005, and 0.010 inches in thickness.

Figure 25 shows the effect of changing the squeeze on the seal. The result is a duo-modal plot of the number of particles of indicated size passing the seal per inch of stroke versus particle size. It is seen that as the squeeze is increased, the number of particulates passing the seal is decreased for all sizes. It is also observed that with increasing squeeze, the lefthand modal plot in Figure 25 experiences an ever-increasing negative slope. This indicates that increasing the squeeze is resulting in a favorability toward the smaller sizes in passing the seal. The righthand modal plot shows a steeper slope for all squeezes up to 6 percent squeeze. This indicates the extreme discrimination against the larger sizes.

Figure 26 shows the percentage of the number of particulates passing the seal which are of the indicated size or smaller for various squeezes. The seal is obviously acting like a filter as
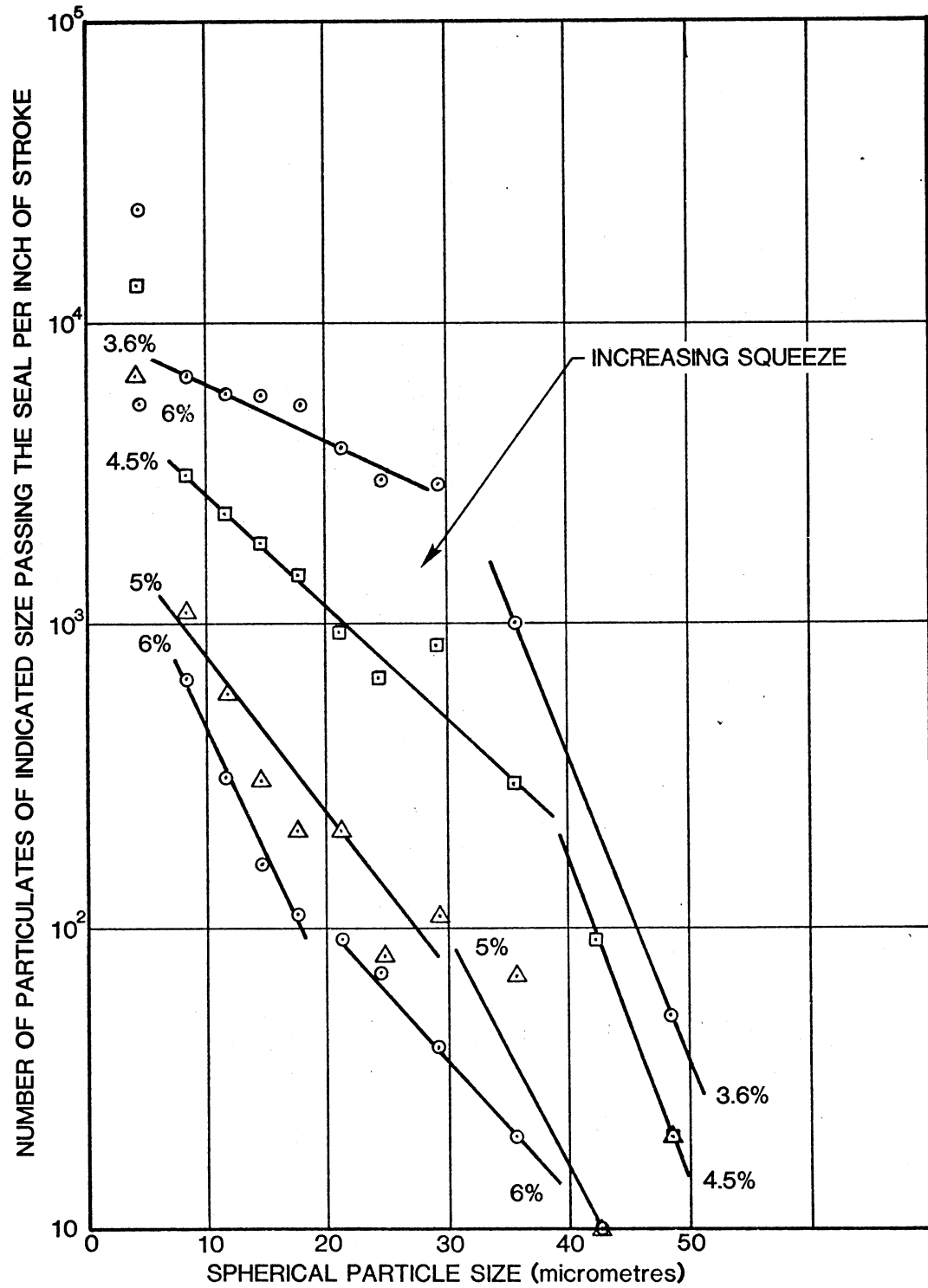
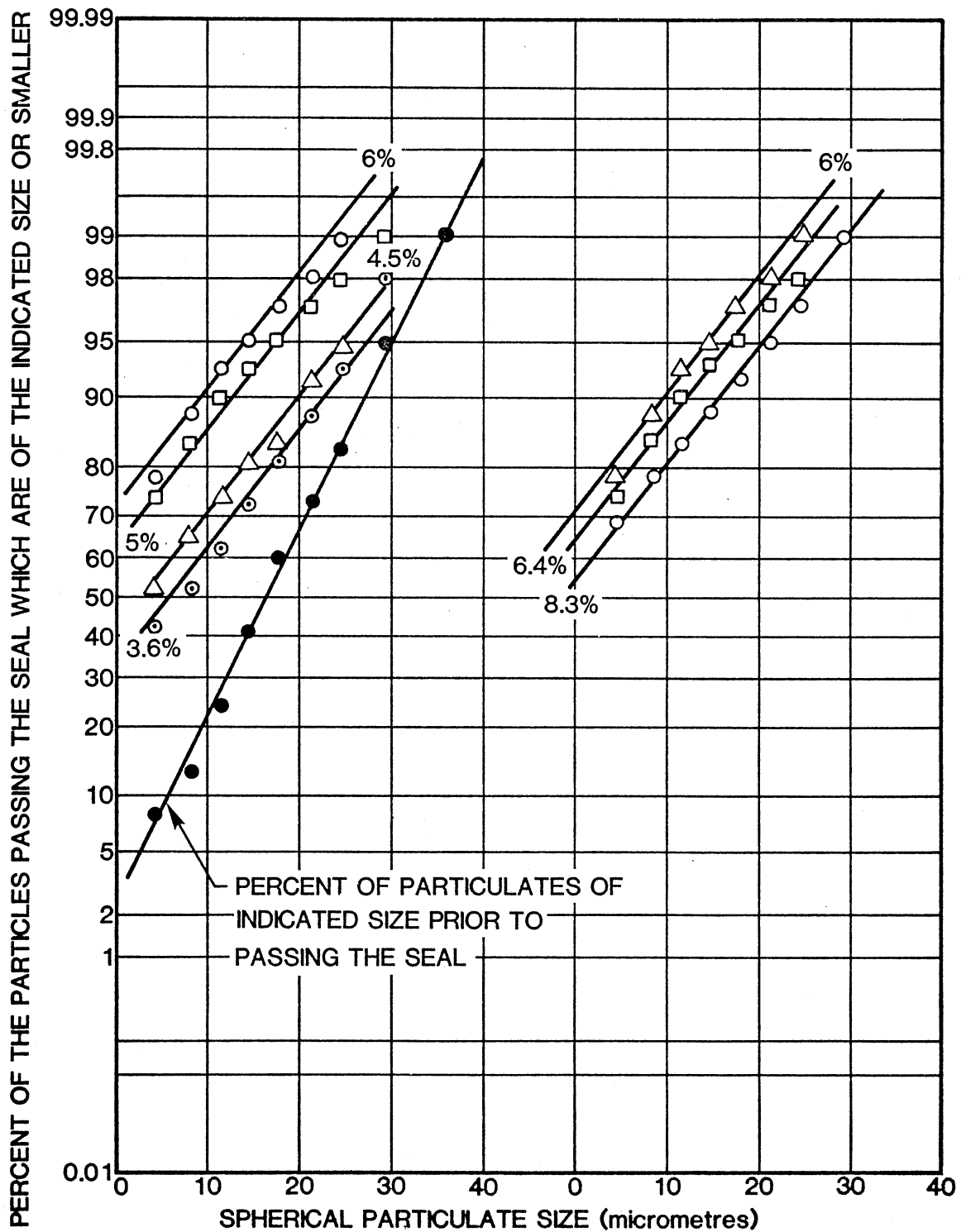Figure 25. Effect of a Changing Entrance Zone Geometry.

Figure 26. The Constant Slope Seal "Filterability" Factor.

can be seen by observing the lower straightline on the lefthand side of Figure 26. The lower line on the lefthand side of Figure 26 is the curve for the spherical particulates prior to passing the seal. The other curves on Figure 26 show the "filerability" of the seal. It is important to note that all the "filterability" curves have the same slope. This denotes that for each squeeze, the seal performs a known precise "sizing" operation on a given particulate population as a function of squeeze. It appears that for the particular seal used in arriving at Figure 26, a squeeze of 6 percent results in the highest constant slope curve. Squeezes above and below 6 percent yield lower constant slope curves.

The effect of elastomer relaxation time on particulate passage is shown in Figure 27. The curves verify the proposed relationship between the number of particulates of a given size passing the seal and elastomer relaxation time as shown in Figure 27. The inverted characteristics bell-shaped curve is seen to occur for particulates in the 4.25 micrometre-size range. As particle size increases, it is seen that the relaxation time corresponding to the minimum number of particules of that size passing the seal decreases. Also, as particle size increases, the number of particles of that size passing the seal increases more rapidly with relaxation time once having passed through the relaxation time corresponding to the minimum number of particles passing the seal.
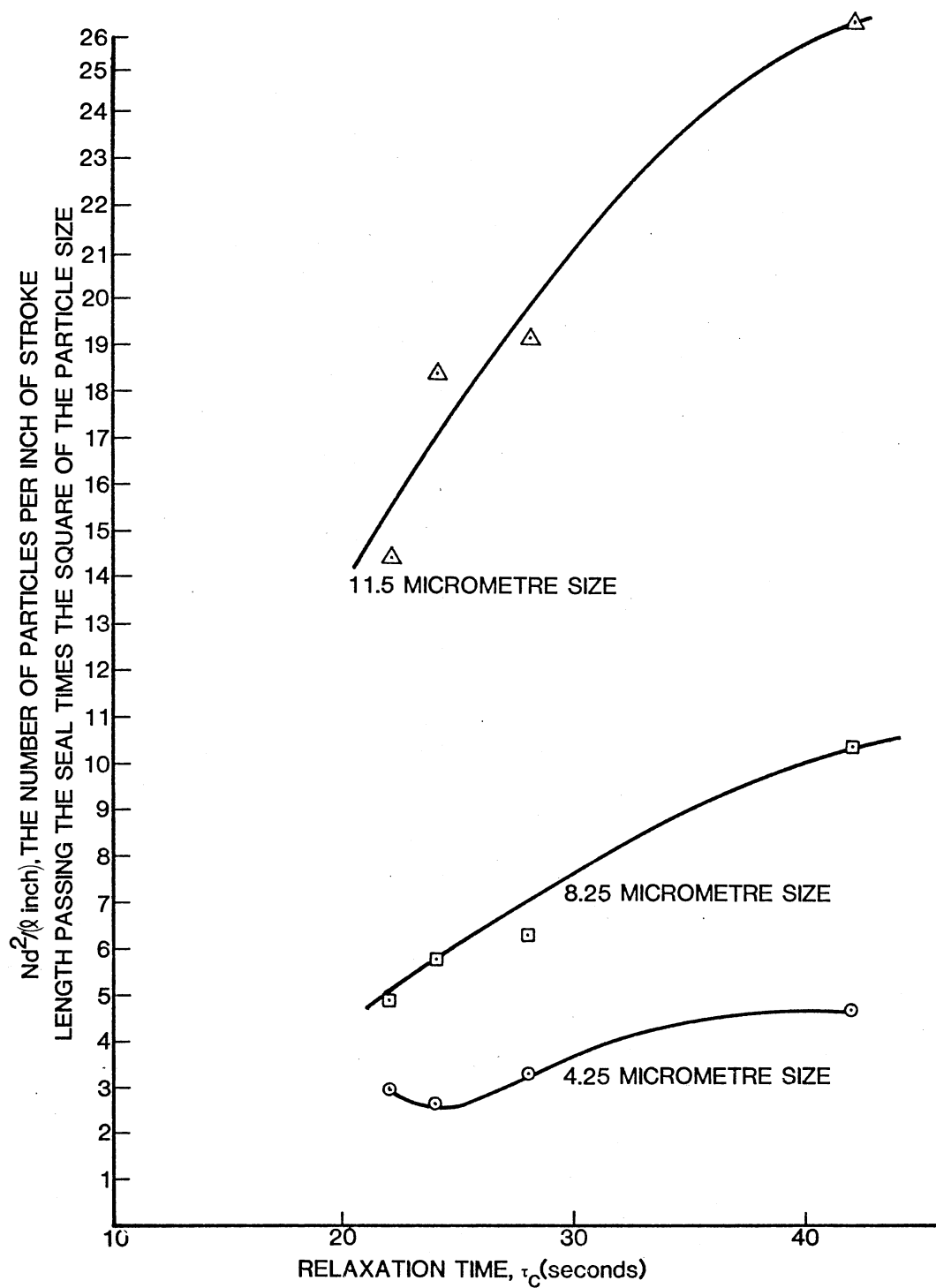
Figure 27.   The Effect of Elastomer Relaxation Time On Particulate
Ingression.

CHAPTER X

CONCLUSIONS

The purpose of this thesis was that of explaining the mechanism whereby particulates are able to be transported through the interface between an elastomer which is pressed firmly onto a hard metal mating surface.

Two main problems were addressed. One of these problems was that of explaining the effect of the entrance zone of a linear elastomeric seal on its ability to exclude particulates brought into intimate contact with it during relative motion between the elastomer and its mating surface. The effect of the slope of the elastomer at its point of initial contact with a particulate was shown to be extremely important. Depending on the coefficients of friction between particulates and the metal mating surface and between particulates as well as the effects of capillarity due to the presence of a liquid, it was shown that elastomer geometry in the entrance zone region determined whether or not particulates were able to be moved from one side of a seal to the other.

It was experimentally determined that there is a precise relationship between a seals "filterability" and the particulate population it is required to work against. The effect of the entrance zone geometry of a seal was shown to heavily discriminate

against larger size particles in favor of smaller size particles. An experimentally determined plot of the number of particulates passing a seal versus particle size for a given particulate population was shown to be a duo-modal plot having two distinct slopes for each entrance zone geometry change. One slope applied to smaller size particulates and the other to larger size particulates.

The percentage of the number of particles of a given size or smaller passing a linear seal was shown to be represented by a straight line of constant slope on probabilty paper for each change in entrance zone geometry. This shows conclusively that seals have a filterability similar to the standard filter rating techniques.

The effect of viscoelasticity on particulate ingression was correctly predicted by theory and verified by experiment. Elastomer relaxation time was shown to be an important parameter in the ability of a linear elastomeric seal to exclude particulates. That there is a relaxation time which will allow a minimum number of particulates to pass through the elastomer mating surface interface was demonstrated experimentally.

Recommendations for Further Study

It is recommended that the effect of non-uniformly shaped particulates on particulate ingression past elastomeric linear seals be assessed. This is extremely important as real world particulates are generally not spherical.

The fatigue mechanism of particulates moving about on elastomers is in need of explanation. This is very important as the "cutting" of seals by particulates has been identified as a major source of seal degradation.

REFERENCES CITED

1. Beakbane, H. R., Seals Handbook, Chapter 4, "Exclusion Devices," Published in the U.S. by Morgan-Grampian Ltd. (1969).

2. Isengarger, R. O., "Seal Devices for Exclusion of Foreign Material from Hydraulic Mechanisms," National Conference on Industrial Hydraulics, pp. 207-222 (date unknown).

3. Jagger, E. T., "The Role of Seals and Packings in the Exclusion of Contaminants," Paper No. 26, Vol. 182, Pt. 34, Proceedings of the Institution of Mechanical Engineers (1967-68).

4. Flock, H. H., and I. L. McMillen, "Rod Scrapers for Earth Moving Equipment," Paper No. 700131, Automotive Engineering Congress, Detroit, Mich., Society of Automotive Engineers (January 12-16, 1970).

5. Nau, B. S.,"Flow in Rod Seal Films and Other Fine Clearences in Relation to Hydraulic System Contamination," Contamination in Fluid Power Systems, Institute of Mechanical Engineers Conference Publications (1976-77).

6. Fitch, E. C., Effectiveness of Contaminant Exclusion Devices, Paper No. 730436, Earthmoving Industry Conference, Central Illnois, Section, Peoria, Ill., Society of Automotive Engineers (April 2-4, 1973).

7. Howsden, J. M., and R. K. Tessman, "Environmental Influences Upon Wiper Seal Performance," Paper No. P75-5, Fluid Power Research Conference, Oklahoma State University, Stillwater, Okla. (October 7-8, 1975).

8. Howsden, J. M., and R. K. Tessman, "Service Life of Wiper Seals," Paper No. P76-31, Fluid Power Research Conference, Oklahoma State University, Stillwater, Okla. (October 5-7 1976).

9. Mitchell, R. J., (ed.), Parker Packing Engineering Handbook, Parker Hannifin Corp. pp. 1-10 to 1-12 (1976).

10. Bensch, L. E., and E. C. Fitch, "Rod Seal Sensitivity to Contaminant Wear," Presented at the 29th National Conference on Fluid Power, Cleveland, Ohio (1973).

11. Zimon, A. D., Adhesion of Dust and Powder, Trans. from Russsian by M. Corn, Plenum Press, N.Y. (1969).

12. Tabor, D., "The Mechanism of Rolling Friction," Proceedings of the Royal Society of London, Series A, Vol. 229 pp. 198-220 (April-May, 1955).

13. Tabor, D., "The Mechanism of Rolling Friction," The Philosophical Magazine, Vol. 43, Series 7, pp. 1055-1059 (January-December, 1952).

14. Tabor, D., "The Mechanism of 'Free' Rolling Friction" Journal of the American Society of Lubrication Engineers, pp. 379-386 (1956).

15. Greenwood, J. A., H. Minshall, and D. Tabor, "Hysteresis Losses in Rolling and Sliding Friction," Proceedings of the Royal Society of London, Series A., Mathematical and Physical Sciences, Vol. 259, pp. 480-507 (January, 1961).

16. Tabor, D., "Elastic Work Involved in Rolling a Sphere on Another Surface," British Journal of Applied Physics, Vol. 6, pp. 74-81 (March, 1955).

17. Norman, R. H., "The Rolling Friction of Cylinders on Planes," British Journal of Applied Physics, Vol. 13, pp. 358-361 (1962).

18. May, W. D., E. L. Morris, and D. Atack, "Rolling Friction of a Hard Cylinder over a Viscoelastic Material," Journal of Applied Physics, Vol. 30, pp.1713-1724 (November, 1959).

19. Halaunbrenner, J. and A. Kubisz, "Contact Region of a Hard Ball Rolling on a Viscoelastic Plate," Journal of Lubrication Technology, Vol. 90, Section 2, pp. 101-105 (January, 1968).

20. Flom, D. G., and A. M. Bueche, "Theory of Rolling Friction for Spheres," Journal of Applied Physics, Vol. 30, No. 11, pp. 1725-1730 (November, 1959).

21. Moore, D. F., The Friction and Lubrication of Elastomers, Chapters 4 and 8, Pergaman Press, N.Y. (1972).

22. Treloar, L. R. G., The Physics of Rubber Elasticity, Oxford at the Clarendon Press, pp. 71, 209-211 (1949).

23. Pao, Yoh-Han, "Extension of the Hertz Theory of Impact to the Viscoelastic Case," Journal of Applied Physics, Vol. 26, No. 9, pp. 1083-1088 (September, 1955).

24. Mase, G. E., _Continum Mechanics_, Schaum's Outline Series McGraw-Hill Book Co., Chapter 9, "Viscoelasticity," pp. 196-206 (1970).

25. Bridgman, P. W., _Dimensional Analysis_, Yale University Press, Rev. Ed., Second Printing (October, 1937).

26. Giles, R. V., _Fluid Mechanic and Hydraulics_, pp. 57-58, McGraw-Hill Book Co., N.Y. (1962).

27. Holman, J. P., _Experimental Methods for Engineers_, Second Ed., pp. 6-77, McGraw-Hill Book Co., N.Y. (1971).

28. Liu, B. Y. H., and V. A. Marple, _Laboratory Manual For Basic Instrumentation_, Vol. 1 (M.E. 3-701, Measurements Lab. I), pp. (9-1)-(9-7), Mechanical Engineering Dept., University of Minnesota (1976).

29. _O Ring Handbook_, Parker Hannifin Corp. O-Ring Division, 2360 Palumbo Drive, Lexington, Ky., Revised Edition (December, 1977).

30. _Vulcanized Rubbers--Determination of Hardness, (Hardness Between 30 and 85 IRHD)_ International Standard, ISO 98-1975 (E) (1975).

31. _Operators Manual_, HIAC Criterion Automatic Particle Size Analyzer Model PC-320, Pacific Scientific Company (date unknown).

$\mathcal{V}$

VITA

Dean Harold Ahlberg

Candidate for the Degree of

Master of Science

Thesis: PARTICULATE INGRESSION PAST ELASTOMERIC VISCOELASTIC
LINEAR MOTION SEALS

Major Field: Mechanical Engineering

Biographical:

Personal Data: Born in Minneapolis, Minnesota, May 2, 1956,
the son of Mr. and Mrs. M. E. Ahlberg.

Education: Graduated from Thomas Alva Edison High School,
Minneapolis, Minnesota, in June, 1974; received the
Bachelor of Mechanical Engineering detree from the Univer-
sity of Minnesota in 1978; completed the requirements for the
Master of Science detree at Oklahoma State University in
December, 1980.

Professonal Experience: Co-operative Engineer, Eaton Corporation
(Char-Lynn), 1976-1978; Graduate Research Assistant, Fluid
Power Research Center, Oklahoma State University, 1979-1980;
Professional Staff Engineer, Fluid Power Research Center,
Oklahoma State University, 1980-present.

Professional Societies: American Society of Mechanical Engineers;
American Society of Lubrication Engineers; National Society
of Professional Engineers; Oklahoma Society of Professional
Engineers.